UNIVERSITÀ DEGLI STUDI DI PADOVA

Dipartimento di Scienze Farmaceutiche

SCUOLA DI DOTTORATO DI RICERCA IN :

Biologia e Medicina della Rigenerazione

INDIRIZZO : *Ingegneria dei Tessuti e Dei trapianti*

CICLO : XX

INTEGRAZIONE DI FORZE MECCANICHE, FATTORI CIRCOLANTI E MATRICI EXTRACELLULARI: UN NUOVO PARADIGMA IN INGEGNERIA DEI TESSUTI

Direttore della Scuola : Ch.mo Prof. Pier Paolo Parnigotto

Supervisore : Ch.mo Prof. Francesco Mazzoleni

Correlatori : Prof. Dennis P. Orgill

Prof. Amy J. Wagers

Prof. Donald E. Ingber

Prof. John Vournakis

Dottorando : Giorgio Pietramaggiori

A mia Madre, che credendo in me mi ha fatto diventare grande

A Saja, che mi ha fatto vedere tutto con occhi diversi

A Giuliano, un vero leone

A Boston, dove Scott, Dipak, Paolo, Arja, Sui, Mike,Alberto&Isa, Jass, Don, Amy, Dr. Valeri, Dr. Vournakis, DO, Dr. Yannas, Dr. Murray hanno incrociato la mia via per sempre

Index

Integrazione di forze meccaniche, fattori circolanti e matrici extracellulari: un nuovo paradigma in ingegneria dei tessuti

BREVE RIASSUNTO

Nuove strategie terapeutiche sono necessarie per fronteggiare il drammatico aumento della prevalenza di ulcere di difficile trattamento.
Utilizzando nouvi modelli in vivo ed un sistema di staging della guarigione svillupato ad hoc, in questi studi proponiamo un importante ruolo di forze meccaniche come stimolatori, non farmacologici, della guarigione.
I risultati dimostrano che l'utilizzo di regimi controllati di forze tensorie in vivo possono, da soli o in combinazione con i piu' tradizionali aprocci basati su matrici extracellulari e fattori solubili, essere utilizzati clinicamente per aumentare la proliferazione epiteliale e rimodellare il letto microcircolatorio cutaneo.

Mechanical forces, circulating factors and extracellular matrices: a new paradigm in tissue engineering

MINI ABSTRACT

New therapeutical strategies are needed to face the dramatic increases in the prevalence of difficult to heal ulcers.
Using new in vivo models and a wound staging system developed ad hoc, in these studies we propose an important role of mechanical forces as non pharmacological healing inductors.
Results demonstrate that controlled regimens of mechanical forces in vivo may be used to stimulate cell proliferation and vascular remodeling, alone or in combination with more traditional approaches based on soluble factors and extracellular matrices.

Sommario

Sommario

Introduzione: L'ultimo decennio è stato caratterizzato da un incremento esponenziale della prevalenza di obesità e diabete di tipo 2, nell'ambito di una popolazione mondiale in costante invecchiamento. Parallelamente a questi fenomeni epidemiologici è aumentata la prevalenza di ulcere croniche.
L' approccio terapeutico nei confronti di questi difetti tissutali sta radicalmente cambiando e nuove affascinanti ipotesi delineano la possibilità di utilizzare induttori non farmacologici di proliferazione cellulare, quali forze meccaniche, al fianco dei più tradizionali approcci terapeutici.

Obiettivo: In questi studi, svolti in collaborazione con l'università di Harvard (Boston), descriviamo un nuovo paradigma terapeutico per ferite difficili basato sulla combinazione di fattori circolanti, matrici extracellulari e forze meccaniche.

Risultati: Gli esperimenti sono stati effettuati utilizzando due modelli animali principali: per le ferite è stato impiegato il topo diabetico (db/db), su cui sono state inflitte ferite dorsali (1 cm^2) a tutto spessore; per lo studio delle forze meccaniche e' stato sviluppato un modello nel quale orecchie di ratto sono state sottoposte a diversi regimi tensori.
L'analisi dei risultati è stata effettuata con un sistema di staging della guarigione basato su vascolatura e proliferazione cellulare sviluppato ad hoc.
Per caratterizzare l'importanza dei fattori circolanti nell'induzione della guarigione, il modello animale è stato ingegnerizzato: topi diabetici sono stati uniti in parabosi a topi singenici normali (wild type) per formare una chimera con costante scambio di sangue tra i due. Entrambi gli animali hanno poi subito ferite sperimentali a tutto spessore che sono state studiate nel tempo. Controlli, in questo caso, sono state coppie parabiotiche costituite da due topi diabetici e due topi normali.
Ferite su topi diabetici costantemente esposte ad elementi circolanti provenienti dal topo normale hanno mostrato un miglioramento nella guarigione, con incrementi di

vascolarizzazione e proliferazione cellulare rispetto ai controlli, mentre sorprendentemente la glicemia è rimasta inalterata.

Sostituti della matrice extracellulare sono elementi fondamentali per indurre la rigenerazione di ferite a tutto spessore. Sostituti dermici costituiti da matrici extracellulari porose simili al derma per struttura (fibre intrecciate con orientamento semi-casuale) e composizione chimica (collagene e condroitin-6-solfato), applicate su ferite a tutto spessore sperimentali, si sono integrate nelle ferite, mostrando precoce ripopolazione da parte di un alto numero di cellule provenienti dalla circolazione. Le cellule attecchite nelle matrici hanno mostrato un fenotipo prevalentemente infiammatorio, mentre scarso è stato il contributo da parte di cellule endoteliali, che ha corrisposto ad una limitata rivascolarizzazione.

I fattori di crescita sono elementi solubili espressi durante la guarigione. Per studiare l'effetto di fattori di crescita, Vascolar Endothelial Growth Factor (VEGF) ricombinante, potente fattore angiogenetico, implicato nella crescita tumorale, è stato applicato su ferite in animali diabetici. Risultati hanno dimostrato la capacità di questo fattore di stimolare notevolmente (>10 volte) l'angiogenesi, ma non la proliferazione cellulare, inducendo la formazione di un tessuto cicatriziale imaturo.
L'utilizzo di piastrine concentrate, combinando fattori di crescita ad un sistema di somministrazione cellulare, hanno stimolato più di due volte la vascolarizzazione e più di quattro volte la proliferazione cellulare, rispetto a controlli non trattati, determinando la formazione di un tessuto cicatriziale compatto.
Per sorpassare le limitazioni dei fattori di crescita (azione molto limitata nel tempo ed effetto molto selettivo) e dell'uso di piastrine (che necessitano di particolari preparazioni ex-vivo), è stato utilizzato un polimero altamente acetilato (poli-N-acetil glucosamina, NAG) che interagisce specificamente con le piastrine circolanti amplificandone l'attivazione. Ferite trattate con NAG hanno dimostrato stimolazione di vascolatura e proliferazione cellulare simile a quella indotta da piastrine.

La mecanotrasduzione è la trasformazione di uno stimolo meccanico in stimolo chimico di proliferazione. Questo meccanismo è possibile a livello cellulare perché l'organizzazione del citoscheletro cellulare è assimilabile alle sculture di Tensegrity,

descritte da Snelson e Fuller in architettura, che mantengono un equilibrio ad alta energia grazie a strutture in “continua tensione” (nelle cellule i microfilamenti) embricate con strutture soggette a “compressione localizzata” (nelle cellule i microtubuli). Essendo queste strutture tutte collegate in un equilibrio dinamico ad alta enargia, deformando la loro struttura applicando forze meccaniche alle cellule in vitro è possibile stimolare la loro funzione, attuando appunto mecanotrasduzione.
Orecchie di ratto sottoposte a tensione meccanica continua hanno evidenziato un incremento graduale della proliferazione epiteliale culminato dopo due giorni. Il letto microcircolatorio cutaneo ha subito una dilatazione a seguito dell'applicazione della tensione, ma la proliferazione delle cellule endoteliali non è stata stimolata rispetto ai controlli. Sorprendentemente, regimi tensori ciclici hanno dimostrato la capacità di stimolare la proliferazione epiteliale cellulare molto più velocemente rispetto a regimi continui (nell'ambito di otto ore).

Il modello clinico utilizzato per combinare forze meccaniche, matrici extracellulari e fattori circolanti è la Vacuum Assisted Closure device (VAC), costituita da una interfaccia porosa di poliuretano compressa sulla superficie della lesione mediante medicazione sottoposta a pressione sub-atmosferica. I risultati hanno dimostrato come questo congegno trasmetta forze meccaniche mediante microdeformazioni tissutali e stimoli la proliferazione cellulare in ferite sperimentali su topolini diabetici, mentre l'interfaccia di poliuretano non è in grado di integrarsi nella ferita ed induce un effetto angiogenetico per reazione da corpo estraneo.
Per stimolare la guarigione ed indurre rigenerazione al contempo, all'interfaccia di poliuretano della VAC è stata sostituita una matrice porosa biodegradabile e biocompatibile di NAG, che sotto l'effetto di regimi ottimizzati di pressione sub-atmosferica ha rapidamente stimolato angiogenesi e proliferazione cellulare.

Conclusioni: I risultati hanno dimostrato che matrici extracellulari, fattori solubili e forze meccaniche da soli o in combinazione svolgono un ruolo specifico di induzione di proliferazione cellulare o angiogenesi e, rappresentano un nuovo paradigma, clinicamente rilevante, in ingegneria dei tessuti.

Abstract

Introduction: The last decade has been characterized by an esponential rise in the prevalence of obesity and diabetes type 2 in the context of the world's aging population. Along with these epidemiological trends, chronic ulcers increased in a parallel fashion.
The terapeutical approach to face these tissue defects is radically changing. New intriguing hypothesis have been postulated on the use of non pharmacological inductors of cell proliferation, such as mechanical forces, to flank the more traditional ones.

Objective: In these studies, performed in collaboration with Harvard University (Boston), we descibe a new terapeutical paradigmto treat difficult to heal wounds based on the combination of circulating factors, extracellular matrices and mechanical forces.

Findings: The experiments have been performed using two main animal models: to study wound healing, we created full-thickness wounds ($1cm^2$) on the dorsum of the diabetic (db/db) mouse; for the study of the effects of the mechanical forces, we developed a rat ear stretch model.
A wound healing staging system developed ad hoc and based on vascularity and cell proliferation was used to compare the results.
To characterize the importance of soluble, blood borne factors, in healing, we engineered the animal model: diabetic mice were joined in parabiosis to wild type mice to form a chimera with constant exchange of blood between the two. After parabiosis was established, both animals received the standardized full thickness wounds on the back that were studied over time. Controls were parabiotic couples between two diabetic and two wild type animals. The wounds on diabetic mice exposed to wild type peripherical circculation showed improved healing characterized by increases in vascularization and cell proliferation compared to controls, while surprisingly glycemia remained unchanged.

Extracellular matrix substitutes are crucial to induce regeneration of full-thickness wounds. Porous extracellular matrices similar to dermis in structure (randomly oriented fibers) and chemical composition (collagen and chondroitin-6-sulphate) grafted on full-thickness wounds showed complete integration and colonization from circulating cells. Engrafted cells in the matrices showed an inflammatory phenotype, while scarce was the endothelial cell repopulation, corresponding to slow revascularization.

Growth factors are soluble elements secreted during repair. To study the effect of growth factors, Vascular Endothelial Growth Factor (VEGF), potent angiogenic factor, involved in tumor growth, was applied on full-thickness wounds on diabetic mice. Results showed that VEGF stimulated angiogenesis (>10-fold increase) but not cell proliferation, inducing the formation of immature scar tissue.
The use of platelet rich plasma (PRP), combining growth factors with a cellular drug delivery system, induced a more symmetric stimulation: 2-fold increase in vascularity and a 4-fold increase in cell proliferation compared to controls, leading to a more compact scar tissue.
To overcome the limitations correlated to the use of growth factors (very short acting and selective activity) and platelets (requiring ex-vivo manipulations), we utilized a highly acetylated polymer (poly-N-acetyl glucosamine, NAG) that specifically interacts with endogenous platelets amplifying their activation. Wounds treated with NAG patches showed increases in vasculature and cell proliferation comparable to PRP.

Mechanotrasduction is a mechanism that transforms a mechanical stimulus into a proliferative chemical one. This mechanism is possible because the organization of the cytoskeleton of the cells resembles the tensegrity sculptures, first described by Snelson and Fuller, in architecture. These sculptures have a very high energetic level due to structures subjected to “continue tension” (in the cells the microfilaments) and “local compression” (in the cells the microtubules). Being these structures all connected and highly reactive, a deformation of their shape results in a change of their function, which is the mechanotrasduction.

Rat ears, subjected to continuous mechanical tension, showed a gradual increase in epithelial proliferation peaking after two days. The diameter of the vessels in the issues subjected to forces increased, but endothelial cell proliferation was not noticed. Surprisingly, when cyclical regimens of tension where applied, they induced a much faster stimulation of cell proliferation compared to continuous tension (within 8 hours).

The clinical model adopted for the combination of mechanical forces, circulating factors and extracellular matrices was the Vacuum Assisted Closure device (VAC), which is a polyurethane, open pore sponge compressed on the wound surface by a semipermeable dressing subjected to sub-atmospheric pressure. Results showed how this device transmits mechanical forces through tissue microdeformations corresponding to increases in cell proliferation in standardized wounds on the diabetic mice. The polyurethane interface may have acted as a foreign body aspecifically stimulating angiogenesis.
To stimulate wound healing while modulating regeneration at the same time, we developed a NAG-based wound interface (biodegradable and biocompatible) with regenerative characteristics. This interface was applied under optimized regimens of sub-atmospheric pressure and stimulated cell proliferation and rapid revascularization.

Conclusions: Results demonstrated that extracellular matrices, soluble factors and mechanical forces individually or in combination have a specific role in stimulating cell proliferation or angiogenesis and represent a new healing paradigm in tissue engineering.

1. Introduction

1.1 Healing of Skin Defects

The large aging population is plagued with an increasing number of acute and chronic, non-healing wounds, mostly due to the surge in type 2 diabetes. Diabetic patients have a 12-25% lifetime incidence of foot ulcers[3] and a 15 times higher risk for foot amputations[4] than non-diabetics. Wounds from complex surgeries, radiation therapy, immunosuppression, severe infections resistant to antibiotics and pressure sores aggravate this medical problem. Taken together, wounds are one of the main challenges for the healthcare system.

A wound is a disruption in the continuity of cells - anything that causes cells that would normally be connected to become separated. Wound healing is the restoration of that continuity. Two are the main mechanisms of healing: regeneration and repair. While regeneration restores the normal structure and function of tissues after injury, repair involves the formation of scar tissue to re-establish integrity. Most adult human tissues have lost their regenerative abilities. In skin, epidermis can regenerate, but not dermis, thus all wounds that penetrate the basal lamina of the epithelium will induce scar formation.[1]

Skin defects fall into two main categories: (1) wounds with approximated edges, healing by “first intention”, such as clean surgical incisions, whose borders are approximated by sutures and (2) wounds with separate edges and substantial skin loss, healing by “second intention”.

The healing process is about the same in both situations, but the latter is characterized by a more intense inflammatory reaction, a larger amount of granulation tissue formation, and, generally a far more significant wound contraction compared to the former.[2]

A wound can close naturally in the due times, or become chronic, depending on many local and systemic factors, such as diabetes, which can influence the healing process.

The normal healing process

Healing is a dynamic process involving the interaction of numerous soluble factors, cells and the extracellular matrix (ECM). It is classically divided in three largely overlapping phases: inflammation (or lag), proliferation (or new tissue formation) and remodelling.

Inflammation begins with injury and continues during the first week. Vasoconstriction and haemostasis are the first events to take place after vasal disruption and extravasation of blood. They follow the **activation of endothelium**, **platelets** and the **coagulative cascade**, in which also a great amount of **soluble mediators** are released. The cloth that is formed serves as a temporary scaffold for invading cells, and also to concentrate cytokines. These substances recruit leukocytes to the site of injury: first neutrophils, which cleanse and sterilize the area and then quickly undergo apoptosis; then they are substituted by monocytes (48 to 96 hours after injury), that become activated macrophages, the cell probably playing the pivotal role in the whole process. Macrophages have a phagocytic activity and stimulate through cytokines keratinocytes, endothelial cells, fibroblasts, being thus essential for the transition to the proliferative phase. The inflammatory phase does not just "burn out" when initiating stimuli are depleted, but is organized as a series of reactions to produce "stop signals".

The *proliferative phase* begins within hours after injury and continues through day 14. It is based on the interaction between **circulating stem cells**, **epithelization**, **angiogenesis**, and **provisional matrix formation**. Epidermal cells from the skin edge and appendages begin proliferating, and lose connection within each-other and the dermis; they migrate centripetally responding to soluble signal factors and interacting mechanically with the ECM, especially with fibronectin. Their migration dissects the eschar on the top (mainly constituted by coagulated blood and dead cells) from the viable tissue on the bottom. Stem cells from the bulges of hair follicles probably do not participate in normal skin renewal, but after injury they migrate into the wound, acquire an epidermal phenotype and contributing to acute repair. The definitive new epidermis shows the presence only of keratinocytes derived from epidermal stem cells from the basal layer of the skin.[5-7]

Four days after injury a new stroma, called **granulation tissue**, begins to form. Endothelial cells of intact veins are induced by **VEGF** and other factors to form new

capillaries, carrying to the wound bed the oxygen and nutrients needed for cells metabolism; VEGF is produced mainly by keratinocytes, under stimuli coming from the other cells involved, included endothelial cells themselves. The capillary sprouts are guided by interaction with ligand of an **integrin receptor** for fibrin/fibronectin expressed on their tips. Fibroblasts and macrophages migrate at the same time, both kind of cells produce the new matrix and are a source for growth factors. PDGF and EGF, derived from platelets and macrophages, are the main signals to fibroblasts. It has been suggested that angiogenesis may precede shortly the fibroblasts invasion. Following this hypothesis, endothelial cells would be responsible for the provisional matrix formation, including fibronectin deposition which guides fibroblasts growth, while fibroblasts would then be responsible for the deposition and remodelling of the collagen matrix which substitutes the provisional one.[8] TGF-β is responsible for the activation of its synthesis (days 7-14), and also for the transformation of fibroblasts in myofibroblasts for wound contraction. Still unknown signals induce cells apoptosis, and the fibroblasts-rich tissue is replaced by a relatively acellular scar. The complex interaction and feedback control of cells, cytokines and matrix has been termed "dynamic reciprocity".

Remodelling takes place from the second week, up to more than years after injury. Myofibroblasts are modified fibroblasts containing large bundles of smooth muscle actin-rich filaments (Alpha-SMA), which in a mechanically-loaded environment, such as a wound, can contract and induce scar retraction. The transition to mature scar is the result of a continued low-rate synthesis and catabolism of collagen, involving the activity of metalloproteinases secreted by macrophages, keratinocytes, endothelium and fibroblasts. The final result is the replacement of the temporary matrix with a stronger and organized one, with a decrease in collagen III proportion from 30% to 10%, like in uninjured skin[9-13].Nevertheless, scars never attain the same breaking strength of uninjured skin, getting to a maximum of 70-80% of it.[10]

Pathologic wound healing

Wound healing can complicate for the action of local and systemic factors.

Main *local factors* are:

1. Infection, stimulus for a prolonged inflammation, which profoundly interferes with all molecular and cellular processes;
2. Foreign body or necrotic tissue, physical obstacles and asylum for bacteria;
3. Ischemia (also related to edema), which obstacles chemotaxis, toxins removal and deprives the wound bed of oxygen, glucose and other supplies needed for such an energy-dependant process characterized by highly increased methabolism.

Systemic factors are:

4. Diseases affecting tissue perfusion and blood oxygenation (cardiac, respiratory);
5. Endocrine and metabolic diseases (such as diabetes mellitus and hypothyroidism);
6. Organ failures (renal, hepatic);
7. Major stress (burns, hypothermia, pain, trauma), leading both to a systemic inflammatory state, diffuse adrenergic discharge with subsequent cutaneous vasoconstriction, eventually also to ipovolemia;
8. Others: age, nutritional state, smoking, corticosteroids (demonstrated inhibitory effect on inflammatory and skin cells).

The process can result abnormal both in defect or in excess of the events taking place in each phase: in the first case we have difficult closure, in the second keloids and hypertrophic scars or contraction.[2, 9, 10, 14-17]

1.2 Wound healing strategies

Conservative and time-honoured care methods should always be attempted first, such as standard wound dressings to induce adequate moisture, débridement, restoration of perfusion, limitation of pressure, control of infection and amelioration of systemic problems.[9, 10]

The simplest and least expensive dressing remains plain gauze and saline (wet to dry dressing), with eventual antibiotic ointment. Its disadvantages are represented by the need of frequent painful dressing changes and dessication and irritation of adjacent skin, but it remains effective for most uncomplicated wounds[9].

In recent years, correlated to the epidemics of diabetes and obesity, the incidence of complicated wounds started rise dramatically and many efforts have been dedicated to finding new, cost-effective strategies for their cure.

In these studies, we characterize the effects of three main healing effectors: circulating factors, regenerative scaffolds and micro mechanical forces.

a. Soluble Factors – Growth Factors and Circulating Cells

High expectations had been placed on growth factors to accelerate and control wound healing, but the clinical experience has been discouraging. Considering the complexity of the interactions taking place in the wound, this is not surprising. It is possible that better results will be reached by the administration of combinations of growth factors at the due time. One of the most promising fields of research is represented by platelets, whose role in wound healing is now being investigated.[9, 10, 18-20] Platelet aggregation initiates coagulation in bleeding vessels[21] and releases growth factors that regulate wound healing events. Platelets carry over 20 growth factors[22] including PDGF-BB, EGF, TGF-_, and VEGF, which have been shown to improve wound healing in healing-impaired animal models and in human chronic wounds.[23-25] Conversely, reduced levels or absence of the same growth factors and some of their associated receptors have been found in difficult to heal wounds.[26,27]
The temporal changes in growth factor concentrations in wound beds are indicative of a complex process involving multiple pathways that orchestrates wound healing. Demonstration of enhanced wound healing through synergistic growth factor application supports this concept.[28] The underlying practical difficulty with designing a multiple growth factor treatment is to predict the proper time-dependent growth factor ratios for optimal healing. An alternative approach is to replicate and possibly enhance the natural response to wounding through the application of platelet-rich plasma (PRP). PRP preparations can concentrate platelets and their growth factors up to 8 times basal levels in whole blood without inducing platelet activation.[29] PRP is currently used in combination with cancellous bone grafts to treat osseous defects and has been used extensively in plastic surgery.[30-32] The use of autologous PRP eliminates the potential for disease transmission and immunogenicity; however, preparation requires time to draw and process patient blood. Furthermore, the quality of autologous platelet preparations is inconsistent due to individual patient characteristics,[33] many of whom have systemic diseases and are debilitated. This inconsistency may explain in part the mixed results seen in clinical studies.[34-37] Healthy, allogeneic platelets may potentially circumvent this problem by allowing process standardization, but current blood-banking standards require platelets to be stored at room temperature and discarded after five days[38] thereby limiting the availability for wound healing applications.

To overcome the storage limitation of autologous PRP preparations it is possible to use alternative approaches to harness the wound healing stimulatory effects of platelets. Highly homogeneous and pure poly-N-acetyl glucosamine (NAG) nanofibers can be isolated by the culture of a marine microalga.[6] NAG patches, which contain microalgal nanofibers (SyvekPatch^{TM}, Marine Polymer Technologies, Danvers, MA), have been characterized as hemostatic agents to control bleeding following catheter removal, and are currently used in interventional cardiology and radiology as non-invasive closure devices.[39, 40]

The N-acetyl glucosamine-containing oligo- and polysaccharides are an important class of glycosaminoglycans, molecules largely represented in the dermis and already used for inhibition of surgical adhesions, relief from joint pain, and for skin replacement in reconstructive surgery.[41-43]

In addition, N-acetyl glucosamine is contained in chitosan, a polymer with demonstrated hemostatic properties.[44] Although based on similar molecules, pGlcNAc and chitosan have structural, chemical, and biological differences; the former is constituted of highly ordered insoluble fibers, while the latter demonstrates a heterogeneous and soluble structure.[45] These structural dissimilarities result in hemostatic differences between the two materials. When compared, NAG patches induced hemostasis in 100% of cases, whereas several chitosan-based patches performed worse than a gauze pad control.[45]

Poly-N-acetyl glucosamine nanofibers interact with platelets, red blood cells and endothelial cells,[46, 47] and accelerate hemostasis through a sequence of events that have been recently demonstrated.[48] Platelets specifically interact with the nanofibers of the pGlcNAc patch and, as a result, their activation is amplified.[49] The activation response includes pseudopodia extension, shape change, integrin complex activation, activation of calcium signaling, phosphatidyl serine exposure on the surface membrane, binding of factor X to platelets and an acceleration of fibrin polymerization kinetics.[49] Upon activation, platelets release growth factors which orchestrate angiogenesis and vascular maturation in the injured site,[50, 51] thus contributing to wound healing.

Diabetics and elderly patients frequently use anticoagulants and difficult to treat wounds often are aggravated by significant bleeding even in the presence of normal clotting parameters. The availability of a dressing that could enhance both clotting and wound healing might represent a significant advance for difficult to treat wounds.

In this study, we compared the effects of recombinant growth factors (VEGF), fresh and lyophilized PRP and the NAG patch on full-thickness wounds in the *db/db* mouse model.

Among soluble factors, also circulating cells should be mentioned. Many cells involved in wound repair appear to become frankly dysfunctional when exposed to a diabetic (i.e., hyperglycaemic) environment in vitro.[109-120] In this study, we tested whether this condition can be rescued in vivo by establishing a novel parabiotic model that enables the constant exchange of peripheral blood between wild type and diabetic animals, primarily through the skin microcirculation. We then used this model to assay the effect of factors derived from a normal peripheral circulation on cutaneous wound repair in diabetic mice.

Our parabiosis model involves surgical joining of the skin of two immunologically compatible animals such that they develop a common, anastomosed, cutaneous microcirculation without immune rejection. Cross-circulation in this low flow model typically is established ~2-3 days after joining, with complete blood mixing achieved ~5-8 days later.[52] Because parabiotic animals are connected solely through their shared peripheral circulation, this model provides a powerful approach to determining whether blood-borne factors (either humoral or cellular) from one animal can modulate cutaneous repair in its partner. This parabiotic approach has been used previously to demonstrate a profound rejuvenating effect of exposure to a young blood circulatory system for age-related deficiencies in skeletal muscle regeneration and hepatic proliferation.[122] Parabiosis also has been employed previously to investigate the pathophysiology of diabetes type 2, and in fact, paved the way to the discovery of leptin.[53] However, in these early studies additional anastomosis of the celiac wall (generating an unique abdominal cavity) resulted in early death from starvation of the wild type partner, likely due to a massive exposure to leptin or mechanical compression of the abdominal cavity.[54] Thus, although parabiosis has been employed for understanding diabetes in the past, no studies have previously used such a model to investigate the specific impact of the systemic environment on diabetic cutaneous repair.

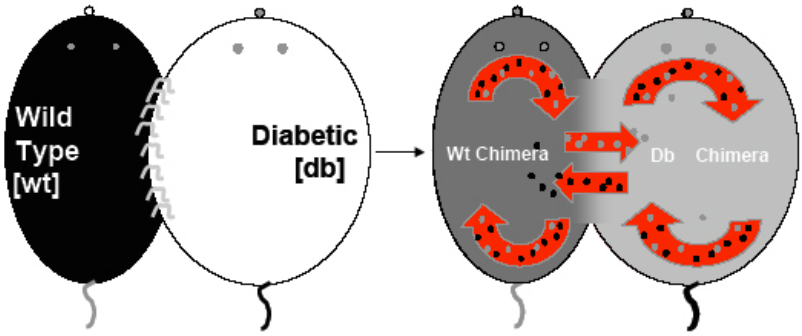

Figure 1. Parabiotic chimera generated from the union of a diabetic and a wild type animal.

To study the effects of blood borne factors on diabetic cutaneous repair, wound healing deficient[125, 126] diabetic mice (*db/db*, hereafter abbreviated db) were joined by parabiosis to normally healing wild type heterozygous littermates (*db/+*, hereafter abbreviated wt). The diabetic mouse served as clinically relevant model of diabetes type 2 in humans,[127, 128] and exhibits defective angiogenesis during wound repair.[94] Following the establishment of cross-circulation in the chimeric couples (db::wt), and in wild type and diabetic control pairs (wt::wt and db::db, respectively), all animals received full thickness dermal wounds, which were monitored for wound healing over 3 weeks, using both morphological and histological metrics of repair.

b. Dermal Regenerative Templates (DRT)

The vast majority of the knowledge about skin regeneration has been developed by Prof. Yannas in the Massachusett Institute of Technology (MIT) between the ’70s and the ’80s. Limb regeneration in certain amphibians is a spectacular feat by which an amputated limb grows back to its original form and recovers its normal function, representing the prototypical paradigm of regeneration. Very few adult amphibians, and none of the adult mammals, can replicate this feat. Instead, the vast majority of mammals, including adult humans, respond to severe injury by a spontaneous repair process.[55, 56] Repair closes the wound by contraction and synthesis of scar tissue without recovery of the uninjured tissues. In contrast, regeneration closes the wound by synthesis of the missing tissues at the original site, yielding a regenerated organ. Regeneration restores the normal structure and function of the organ; repair does not. Spontaneous healing occurs without significant experimental manipulation. In contrast, healing by induced regeneration follows grafting with scaffolds that have high biological activity and are either unseeded or seeded with epithelial cells.[43, 57]

Induced regeneration is the synthesis of nonregenerative tissues in a severely injured adult organ that leads to, at least partial, recovery of physiological structure and function. In clinical terms, it amounts to partial or total replacement of an organ that has stopped functioning due to severe trauma. When an organ can be induced to regenerate, even partially, the patient can be spared most of the problems accompanying alternative procedures that are commonly used.[43] For example, in organ transplantation, the immune response of the host must be suppressed, typically at substantial cost of quality of life or even longevity for the host; in autografting, the donor site contributes significant morbidity, including severe scarring. These problems are obviated by induced regeneration.

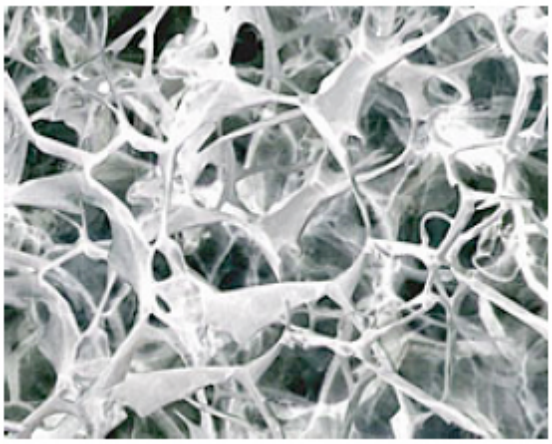

Figure 2. Dermal regeneration templates (DRTs) are highly porous copolymers of type I collagen and chondroitin 6-sulphate (collagen-GAG). The pore size is defined by the processing procedure and averages between 20 and 120 microns. Collagenic scaffolds have a Young's modulus of 200 Pa.

In clear contrast to the adult, the mammalian fetus heals its wounds spontaneously by regeneration, provided that the injury has been inflicted at a sufficiently early stage of gestation, typically before the third trimester. During development healing processes undergo an early fetal to late fetal (often called "adult") transition; the outcome of the transition is a conversion of healing by regeneration to healing by contraction and scar formation (repair).[56] Although not identical to the early fetal response, healing by induced regeneration occurs by minimal contraction and almost no scar formation and is, therefore, clearly distinct from the spontaneous adult healing response. It has been suggested that the fetal response is a sort of "default setting" for healing processes in the organism and that it is partially reactivated when the adult setting is appropriately blocked, as in induced regeneration.[55]

A detailed example of induced skin regeneration, originally described as "artificial skin", has been described elsewhere.[55, 57, 58] The data describe the structural and functional similarities and differences among normal skin, scar and regenerated skin

in the adult guinea pig following grafting of dermis-free defects with the keratinocyte-seeded dermis regeneration template (DRT), a scaffold characterized by unusual regenerative activity. DRT is a macromolecular network synthesized as a highly porous analog of ECM. Among other characteristics, regenerated skin is mechanically competent, fully vascularized and sensitive to touch as well as heat or cold. The regenerated dermal-epidermal junction, with its extensive formations of rete ridges and capillary loops, leaves no doubt that *de novo* regenerated skin organ is clearly not scar. However, regenerated skin differs from physiological skin in the absence of skin appendages (hair follicles, sweat glands, etc.).

Dermal substitutes or matrices are well known to become incorporated with and often indistinguishable from native tissue histologically,[59] producing a pliable and functional skin.[59] Acellular dermal matrices, in both sheet (AlloDerm, Integra) and micronized forms (Cymetra) are increasingly utilized in reconstructive surgery as they serve as scaffolds for the ingrowth of native cellular elements over time. While the sheet form is used for substituting dermal loss, the micronized form - made by freeze-fracturing acellular dermis with a resulting particle size of 100 to 200μm - is used in a paste form to fill complex defects. Early retrospective case studies using these injectable micronized dermal matrices suggest that they may effectively promote healing in refractory ulcers, and recalcitrant sinus tract wounds without surgery and complications, such as rejection or foreign body reaction.[60, 61]

c. Micro Mechanical Forces and cell fate: the tensegrity model

That mechanical forces can influence cell proliferation has long been known. The stretching of cells has been shown to increase proliferation rate both *in vitro* and *in vivo*: in 1968 Lorber and Milobsky showed an increase of tritiated thymidine-labeling of the epidermal cells of the skin of living rats stretched by the insertion of steel pins.[62] MacKenzie described the increase of proliferative rate of epidermidis stimulated by friction,[63, 64] as it had already been observed by Bullogh and Laurence in 1959;[65] stretching of the skin by tissue expansion in a guinea pig was reported by

Francis and Marks to induce an increase of labelling index as well.[66] Stretching of fibroblasts cultured on a fabric mesh was seen to increase the mitotic rate in 1978.[67] Squier, implanting a spring in the back of mice, described in 1980 an hyperplastic response in *in vivo* stretched mouse skin, and in 1981 demonstrated a transformation of fibroblasts in myofibroblasts independently from wounding of the skin.[68, 69] A rapid increase in DNA-synthesizing epithelial cells after mechanical stretching was observed also in vitro by Brunette.[70]

Women's abdominal wall can undergo a large rapid expansion in pregnancy. And in some ethnic groups, tissue growth as a response to stretch has been used to extend anatomical structures far beyond their physiologic commitment.

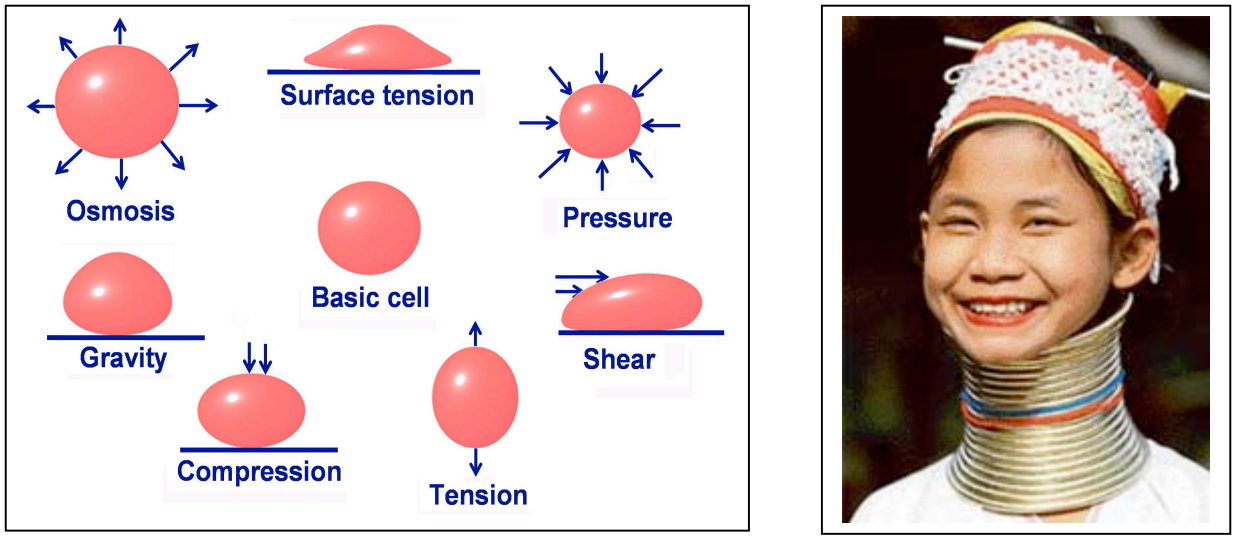

Figure 3. Cells are constantly exposed to forces (left) and it is possible to use mechanical forces to extend natural feature much beyond their natural commitment.

This knowledge has been applied in various fields of surgery, such as orthopaedics, with the Ilizarov's device for distraction osteogenesis (also used to obtain an increased skin surface for the coverage of defects), and in plastic surgery with tissue expanders.

The research performed to study the effects of stretching on epidermis and dermis underneath, showed that, after a first thinning of the skin in the elongation-phase - consistent with its viscoelastic properties - there is a proliferation of the components of the skin with a minimal inflammatory response, resulting in a net gain of tissue with maintained characteristics.[71-75] While the normalization of dermis is described to take up to 2 years, epidermal and vascular proliferation can be seen after a few hours

and is generally accomplished within a few weeks. Moreover, an increase in vascularity of the tissue is reported, which has proved useful to obtain larger surgical flaps with increased survival.[74-82]

Despite this large amount of evidence, there is not yet an agreement on the effects of mechanical forces on cell fate in vivo, and in particular on how cells can sense the stretch and respond undertaking the proliferative pathway. Many hypothesises have been suggested: from the induction of autocrine / paracrine release of growth factors, to the activation of molecular signal pathways inside the cell by stretch-activated ion-channels or membrane force-receptors, as the integrin receptors of the focal adhesions. Experimental data have been collected in support to most of these hypothesis,[83-89] thus suggesting that many different pathways may coexist, all leading to a same result.[90]

The necessity for investigating forces at cellular level began to be felt in the late '70s – early '80s, after original observations by Folkman that occurred while studying tumoral growth control, and suggesting that geometry of the cell seemed to act as gate for growth pathways.[91, 92]

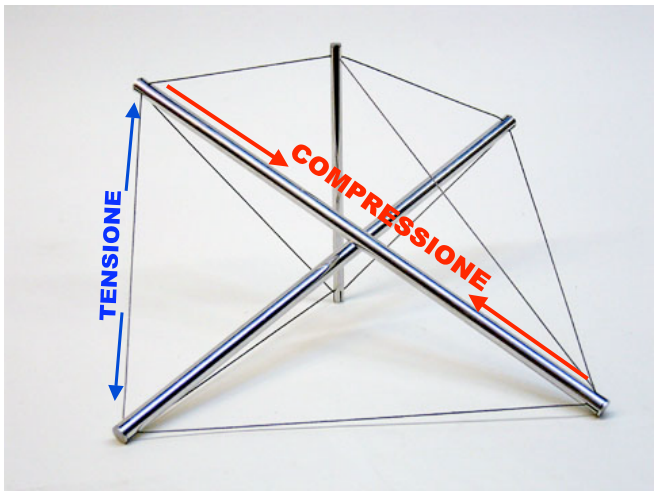

Figure 4. Isolated compressed elements are kept together by a continuous network of elements in tension in Snelson's sculptures.

It soon became clear that the old view of the cell as a "tensed balloon filled with molasses", an elastic membrane surrounding a homogeneous viscoelasic cytoplasm ignoring the internal cytoskeleton, was of little use to the purpose. What was needed was a model allowing to relate mechanics to chemistry and to reproduce in mathematical terms the cell behaviour.

This need induced Folkman and Ingber to investigate a cutting edge theory, called *tensegrity*, which had first been described in the '60s in the fields of art and architecture by K. Snelson and R.B. Fuller.

Snelson developed the concept of a structure made of *incompressible elements (struts)* not touching each-other, and kept together by *taut strings* attached to the ends of the struts (Fig. 4). This creates a *continuous tension network* in which the forces introduced by the tightening are permanently stored in the structure, a state known as *pre-stressing*. With such a structure, which he defined "continuous tension, local compression", simple units can be connected together to create complex structures in which the tension is shared and transmitted between the single elements (Fig. 4). Left to itself, the structure reaches a new equilibrium at the lowest energy status. If a force is applied to any part of it, the structure reacts dinamically and the force is transmitted between the elements that change their reciprocal position gaining a new equilibrium with a new forces balance.[93]

Similar structures can be constructed also without rigid elements, from flexible springs differing in their elasticity.[94]

Fuller, of whom Snelson was a student, had the intuition of further developing this concept, applying it to the geodesic domes he had began to build, thus revolutioning architecture and engineering. While in usual buildings stability is gained through the continuous compression of one brick on the one below, in geodesic domes and in pre-stressed constructions the structure is stabilized by a three dimensional distribution and balance of mechanical stresses. He also coined the name tensegrity, an acronym for "*tensional integrity*" and its most famous definition.[95]

The cell as a tensegrity structure

Linking this engineering model to the structure of cells are many further observations, which have been collected over the past decade. Previous theories assumed that the load bearing system of the cell is the cortical microfilament network beneath the membrane and that the stress is equally borne and transmitted locally in all points of the membrane. Contrasting with this, studies based on magnetic twisting cytometry showed that adhesion receptors such as integrins are specific mechanotransductors;[96-98] and the cytoskeletal lattice to which the integrins provide anchorage to the membrane provides a preferred path for the transfer of mechanical stress into the cell. Also, a local stress applied in one point of the cells membrane (i.e. stretching with micropipettes, magnetic twisting cytometry, or anchoring to a substrate) is followed by rearrangement of the filaments deep inside the cell, up to the other side of it, and by movements and morphologic changes of mitochondria and nucleus, thus resulting

in global structural rearrangements locally and at distance, as the tensegrity theory would predict.[99-101]

From many experiments in which cytoskeleton filaments were selectively disrupted or pre-stress measured and correlated with cellular stiffness, it resulted clear that cells are pre-stressed structures, and that cytoskeleton integrity and pre-stress are major determinants of cell deformability and stability.[94, 96, 99, 102-104]

The cell shape depends on the ability of the substrate to which they adhere through their focal adhesions (FAs) to withstand compression, a plate in vitro, the ECM in vivo, exactly as a muscle needs a bone to withstand compression between its two insertions. Cells also need internal strut elements to refine their shape and extend outward; it may be objected that the same result could be obtained only with tension, but experiments in which the different classes of filaments where singularly disrupted and the effect on the forces exerted on the ECM were measured, revealed that microfilaments and intermediate filaments are under tension, while microtubules bear compression, and biophysical studies showed that they are actually more effective to the one or the other role.[94, 103, 105-107]

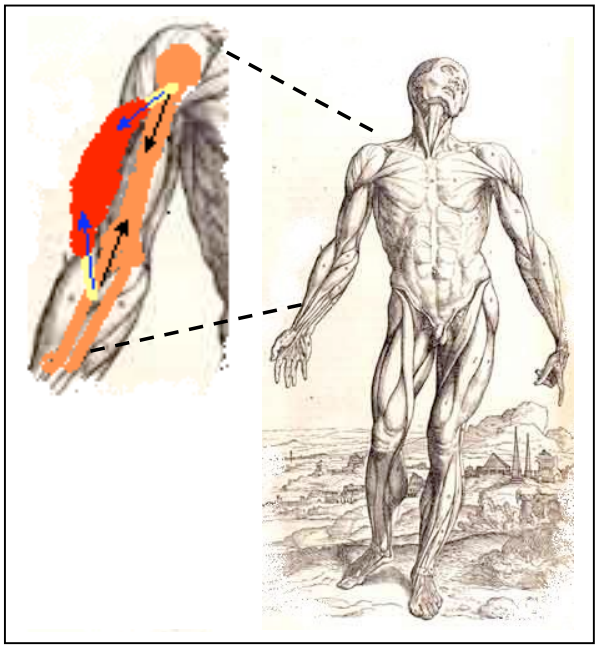

Figure 5. The whole body can be considered a tensegrity structure where compression resistant structures (the bones) are kept together by tensile elements (tendons, ligaments, muscles). Muscles generate the pre-stressed dynamic equilibrium.

In cells, tensional forces are bared by cytoskeletal microfilaments and intermediate filaments acting like elastic strings, and balanced by internal microtubule struts end extra-cellular matrix adhesions that resist compression. However, in different contexts or at different size scales individual filaments can either bear tension or compression. A force equilibrium is established between cytoskeleton components and the ECM.

The primary pre-stress stabilizing the structure is generated by the contractile actomyosin apparatus, and passive contributions to it come from the adhesion to other cells and the ECM and osmotic forces.[94-96]

Like in Snelson's sculptures or Fuller's buildings, the cell would have a *multimodular structure*, meaning that it is composed of smaller self-stabilizing units assembled together; an important consequence of this is that the destruction of one unit (i.e. for replacement) would have only a local effect, and not be followed by the collapse of the whole structure. The tensegrity model may explain the structural stability of nuclei when isolated from their cells, as they may be, in turn, tensegrity structures *integrated hierarchically* into larger ones.

The same principle can be generalized, from small to big, and the whole human body can be interpreted as a hierarchically built tensegrity structure: actually, a body is composed of 206 compression resistant bones kept together by tensile elements (tendons, ligaments, muscles), in a condition of pre-stress generated by the muscles (Fig. 5).[95]

It has been suggested that tensegrity may be the building principle adopted by nature at large.

Mechanical forces and cell behaviour

What is most important, is that the tensegrity model suggests an interesting integrated view of chemical and mechanical signal pathways, in which the mechanical, physical distortion of the cell acts like a filter for the various simultaneous inputs and influences biochemical reactions.[87] It is known that FAs are not only the sites of transmembrane connection between cytoskeletal filaments and ECM or other cells through membrane receptors (integrins, cadherins), but also a site of concentration of molecules (such as receptors, membrane channels, enzymes, co-factors, signaling molecules) implied in many pathways;[90, 108] these molecules are not floating in the cytosol, but bound to the cytoskeleton.[109, 110] In the same way, molecules and organelles of the cytosol are immobilized on the CSK scaffold. Both FAs and CSK are dynamic structures. This means that a mechanical stress can change the relation between the molecules of the cell, influencing the probability of biochemical reactions

to take place; also, changing the architecture of the FA and CSK could alter the shape itself of the molecules bounded to them, thus changing their kinetic and thermodynamic behaviour.[95, 111, 112]

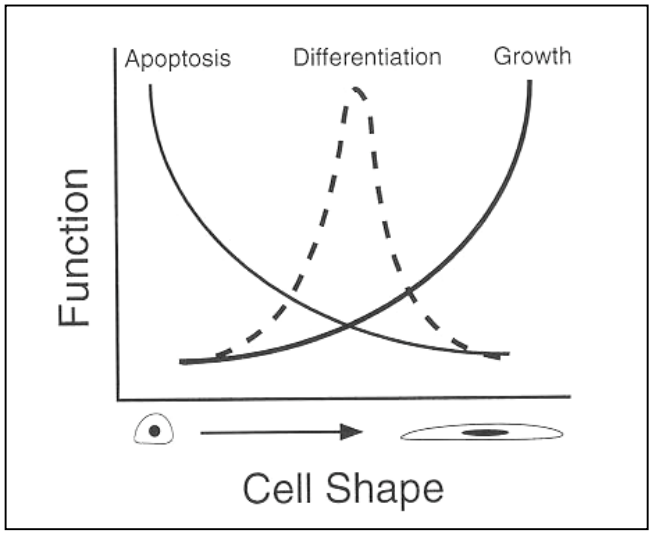

Figure 6. Dr. Ingber identified a relationship (in vitro) between cell shape and cell function. In particular, cells exposed to enough strain to deform their shape tend to grow.

Moreover, experiments in which cell distortion or shape were made the independent variable have shown that, under the same chemical stimuli, the physical state (stretched or unstretched) can be a critical element to switch the cell between opposite gene programs of growth and apoptosis.[108, 113] Adhesion and CSK integrity are required for a cell to transit from G1 to S phase, but even with optimal growth factors and ECM binding, the cell will not enter the S phase unless spreading is also promoted.[95, 113, 114] Local thinning of the basement membrane and the ECM has been demonstrated under the sites of proliferation in the growing buds within developing tissues, resulting in a local mechanic stretch of the cell over it which may increase the cell's ability to undertake the proliferative pathway.[115] Experiments on capillary endothelial cells have shown how the same inputs can produce different functional outputs depending on changing of the force level (and the force balance within the cell) to which the cell is subjected, and in this way it has been possible to shift them from survival to differentiation to growth programs (Fig. 6).[95, 112, 116]

Reconstructive surgeons treat an increasing number of skin tissue defects due to the aging population and the epidemics of diabetes and obesity.[117] Previous attempts to promote wound closure by using growth factors and cytokines to stimulate cell proliferation, motility and angiogenesis have been disappointing[96, 130] possibly

because the physical environment of the wound has largely been ignored. Mechanical tension, for example, plays a critical role in control of cell growth and function, and is important for tissue remodeling in many tissues, including skin.[131, 132] In particular, cell proliferation requires an extracellular matrix (ECM) that physically resists cell traction forces, and increases isometric tension within the cells adherent to it that is required for movement[118] and growth.[114] Numerous *in vitro* studies have established that soluble growth factors cannot stimulate proliferation when cells are adherent to ECM substrates that cannot resist cytoskeletal tension.[88, 134] In the absence of an ECM that can resist cell traction forces, endothelial cells retract, round and become apoptotic.[115] Thus, soluble growth factors must act in concert with ECM and mechanical stimuli to promote cell growth and motility.

Clinical studies with tissue expanders have illustrated the importance of mechanics for tissue development and wound healing.[47, 135] For example, recent findings show that closure of chronic non-healing wounds in humans can be accomplished using a device that exerts mechanical stresses on the healing tissue.[119] This device that is now used clinically applies a vacuum through an open pore foam that is adherent to the wound bed and covered with an occlusive dressing.[120] We recently proposed that the positive clinical results seen in this form of microdeformational wound therapy are caused in part through the application of mechanical forces at the cellular level[35, 136] which we refer to as micromechanical forces. Therefore, application of a moderate external force to intact perfused tissues would be predicted to promote growth of both blood vessels and parenchymal cells within that tissue. Here we test this hypothesis by analyzing the effects of the application of different mechanical force regimens to the ears of living rats.

The Clinical Model of forces in wound healing: The VAC device

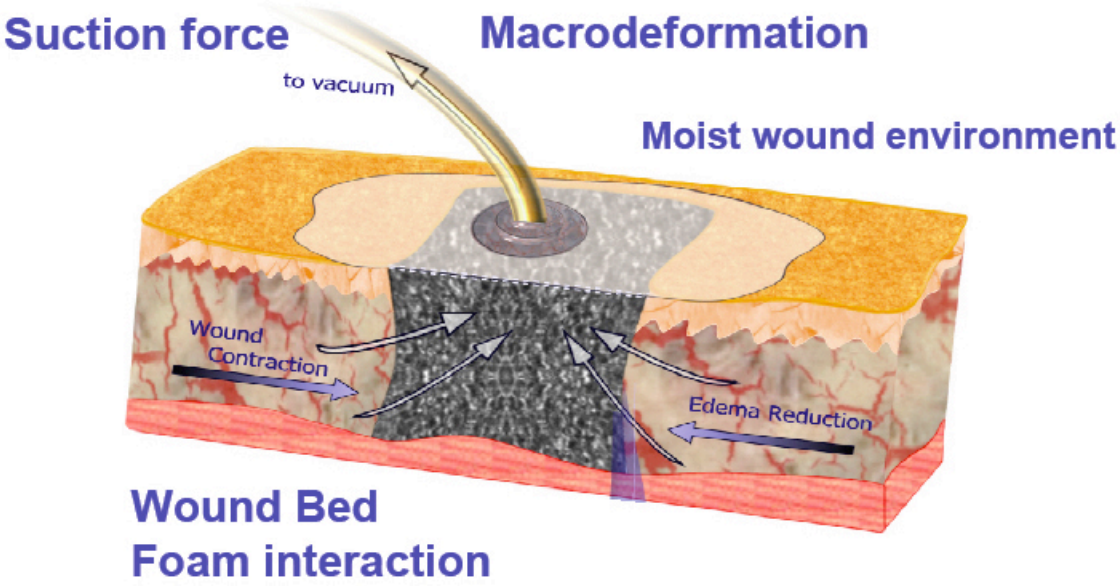

Figure 7. Schematic representation of the VAC.

The device known as VAC (Vacuum assisted Closure device) is a non-pharmacologic wound therapy that was developed less than 20 years ago, and introduced in clinics little over years ago. Since then it became the most common treatment modality for complex wounds in many institutions in North America and in Europe.

The device consists of a porous open-cell sponge in polyurethane or polyvinyl alcohol, which is applied to the wound bed after a good debridement and covered with an adhesive occlusive dressing. The sealed chamber so created is connected with a tube to a vacuum pump, applying a subatmospheric pressure to the dressing. The dressing needs to be changed every 48-72 hours. Up to now, the guidelines suggest an application of a 125mmHg pressure, and even if the device permits both an intermittent or continuous application of the suction, the continuous application for the whole duration of the treatment is recommended for most kinds of wounds (and also preferred by patients as less painful), and for the first 48 hours in all cases.[17, 20, 121, 122]

Originally designed for the treatment of chronic wounds, it has become widely accepted also in the treatment of acute injuries and applied in a wide range of problematic medical and surgical conditions: burns, grafts, diabetic ulcers, orthopaedic traumas, perineal, urologic and gynecologic wounds, fistulae, abdominal wall defects, sternal infections and mediastinitis, up to battlefield contaminated injuries. The only reported limits are that wounds have to be clean and well vascularized.[20, 119]

What has induced such a rapid spreading are the empirical observations on its clinical results and the general impression of cost-effectiveness. Even if contrasting results are found in literature, it is generally reported that the device is less painful and discomforting than traditional treatments, induces a quicker closure of the wound or leads to better results of second-line treatments, while needing less dressing changes, and resulting in reduction of nurse care, hospitalisation time and overall expenses.[17, 20, 121, 123-129]

Since its introduction in clinical practice, notwithstanding the great success obtained, this therapy has gone through little improvements, mainly regarding the combination with other traditional treatments such as the production of a silver-coated foam. The principal obstacle has been the fact that the main mechanism through which the treatment enhances the natural healing process is still unclear.

Many mechanisms of action have been suggested such as *removal of interstitial fluids* with reduction of edema and improvement of perfusion and oxygenation, *removal of inflammatory mediators and toxic molecules* that may affect the normal progression of wound healing, *decrease in the bacterial load* of the wound bed, and more recently *micromechanical stimulation* of the cells in the wound bed.[11, 119, 122, 127, 130]

While the efficacy of the therapy is clinically accepted, the experimental studies on animals and the case reports do not provide definitive evidence to prove a main mechanism of action.[131] For example, many cases have been reported in which only minimal fluid was extracted from the wound bed, without decrease in the positive outcome.[132] Studies on bacterial clearance showed contrasting results; those in which the fluid removed was analysed for signal molecules are inevitably subjected to many bias due to interference of fluid removal itself and heterogeneity of the population. In

addition, the interpretation of the results is difficult and confusing, due to our little knowledge of the many molecular pathways implied in wound healing.[125-127, 130]

In the last few years the attention has shifted to the fourth hypothesis, the effect of the mechanical forces.[127, 130] The evidences presented in the previous paragraphs demonstrate that mechanical stress influences cells proliferation, and strongly support the idea that the relationship may be far closer than previously supposed. Stretching can activate signal pathways and can play a mayor role in inducing individual cells to undertake the proliferative pathway, even independently from soluble factors.

2. Hypothesis and Specific Aims

In these studies we aim to demonstrate that a wound healing paradigm based upon (1) soluble factors and cells, (2) dermal regenerative templates, and (3) micro mechanical forces is a novel, cost-effective strategy to treat recalcitrant wounds.

We will test our hypothesis by demonstrating, in vivo, the efficacy of the elements of the paradigm first alone and then in combination. To characterize the effects of the pivotal elements of the paradigm, we developed novel animal models and a wound healing staging systems.

3. Materials & Methods

These studies are the offspring of the active collaboration between the Plastic Surgery Departments of the University of Padua and of the Brigham and Women's Hospital, Harvard University (Boston). Studies and critical review of the results have been conducted in both Institutions.

Wound Model & Treatment Procedures.

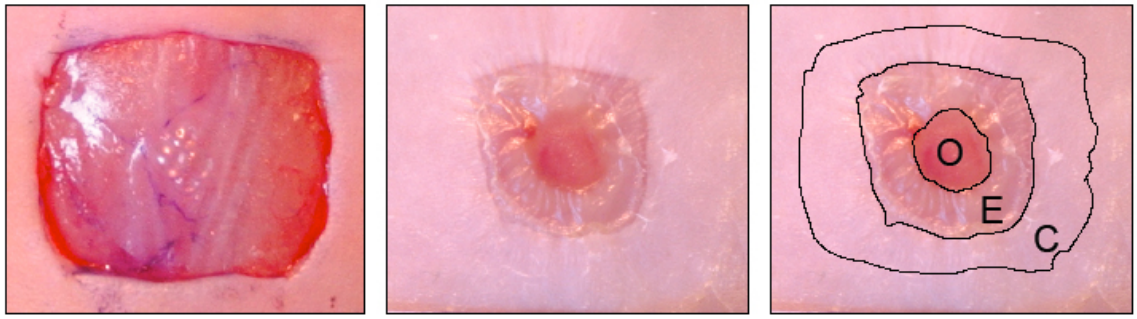

Figure 1. Wound model and wound closure analysis.

Homozygous genetically diabetic 8-12 week-old, Lep/r - db/db male mice (strain C57BL/KsJ-Lepr^{db}) were used under an approved animal protocol in an AAALAC accredited facility. The day before surgery, hair was clipped and depilated (Nair®, Church & Dwight Co., Princeton, NJ). On the day of the surgery, animals were weighed and anesthetized with 60 mg/kg Nembutal (Pentobarbital). A dorsal 1.0 cm^2 area of skin and panniculus carnosus was excised and the wounds were photographed. All wounds were covered with semi-occlusive polyurethane dressing (Tegaderm™, 3M, St. Paul, MN) to maintain a moist wound environment and prevent escar formation. In VAC treated wounds, the edges were covered with a 0.5 cm wide and 0.2 cm thick DuoDERM® (DuoDERM®, CGF®, ConvaTec, Squibb & Sons, L.L.C.) frame to reduce the drastic wound deformations of the wound edges and surrounding loose skin on the back of the animal. Experimental wounds after excision were treated with 1microgram of VEGF165/day for 5 days, with the VAC device for 7 days, with 100microliters of PRP and with 1cm^2 NAG patch.

All treatments started the day of the wounding. On post-operative day 7-10, the animals were euthanized and the wounds were photographed, excised, and fixed in 10% neutral-buffered formalin solution.

Parabiosis.

Parabiotic pairs (experimental chimeras db::wt, wild type controls wt::wt, or diabetic controls db::db; n=8-12 per group) were generated by surgical union of the dorsal and ventral skin along the corresponding lateral surface of age-matched animals as previously described (Fig. 2)[1]. This surgical technique results in low flow peripheral blood exchange through the skin microcirculation, and thus is particularly relevant for the study of systemic factors that may modulate cutaneous healing, which was the main focus of our study.

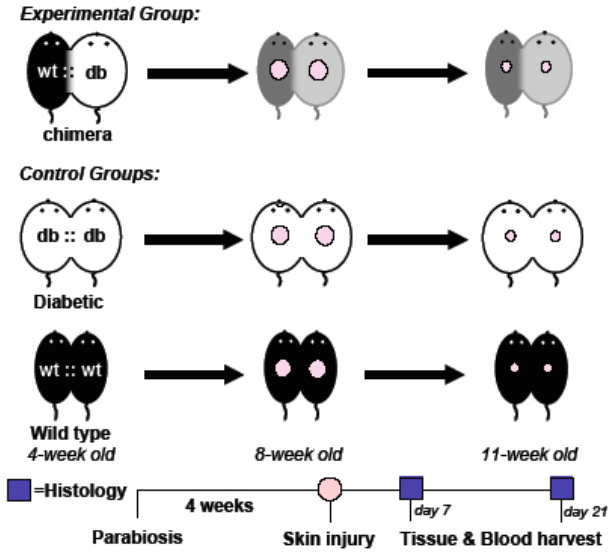

Figure 2. Parabiotic model and wounding scheme.

Assessment of cross circulation.

4 weeks after the parabiosis operation a subset (n=2 couples) of animals from each study condition were used for confirming the presence of cross circulation of blood. One animal in each couple was injected with 100 µl of Evan's blue into the retro-orbital venous plexus. Peripheral blood was collected prior to injection, and 120 minutes post injection, from each animal and serum dye concentration was quantified via spectrometry. Photographs of the animals were taken at 30, 60, 90 and 120 minutes post injection. Once the blood was collected for analysis, random pedicled skin flaps were raised across the junction to visualize blood vessel anastomosis two hours post injection; the concentration of Evan's Blue in the serum of each partner was measured using a NanoDrop spectrophotometer.

30 days after parabiosis operation, each animal in the pair received a dorsal, 0.8 cm^2, full-thickness skin wound[133]. Grafted wounds with collagen gag scaffolds. The day before surgery, hair was clipped and depilated (Nair®, Church & Dwight Co., Princeton, NJ). On the day of the surgery, animals were weighed and anesthetized with 15µl/g of 2.5% Avertin solution and wounds were excised and dressed with a clear semipermeable polyurethane membrane (Tegaderm dressing, Nexcare, 3M, St. Paul, MN). Standardized photographs of all wounds were taken twice a week and wound closure (quantified as reduction of raw area as a percentage of the original wound area, as previously shown [3, 4]) quantified using digital planimetry methods (Image J, NIH, Bethesda, MD) for a total follow-up of 21 days[134]. Tissues were harvested on day 7 or day 21 and wounds with surrounding tissue were harvested en block, fixed in 10% formalin and stored in 70% alcohol at 4°C until central wound cross-sections were embedded in paraffin. Histological cross sections were stained according to routine Hematoxylin and Eosin (H&E) and Trichrome Masson's protocols. Panoramic cross-sectional digital images of each wound were prepared using Adobe Photoshop CS Software (Adobe Systems Incorporated, San Jose, CA). H&E stained sections were analyzed with digital planimetry (Image J, NIH, Bethesda, MD) by two independent observers, blinded to experimental condition, to quantify the area of granulation tissue.

Blood Parameters.

Morning collections of peripheral blood were performed during the follow up. Blood glucose concentration was measured twice a week between 8 and 8:30 AM, using a glucose meter (Lifescan inc., Milpitas, CA). Elisa kits were used to measure plasma Insulin, Leptin (Crystal Chem Inc, Downers Grove, IL) and TNF-_ (Invitrogen, Carlsbad, CA) and cholesterol levels with an enzymatic-colorimetric system (Stanbio Laboratory, Boerne, TX).

Flow cytometry of peripheral blood.

One day after wounding, peripheral blood was collected from the tail vein of each animal in each experimental condition. Nucleated peripheral blood leukocytes were isolated from whole blood following ammonium chloride-mediated lysis of red blood cells (RBC). Cells were then stained using a cocktail of antibodies to detect blood

lineage markers (including CD3 (145-2C11, Cy7PE conjugate), CD4 (GK1.5, Cy7PE conjugate), CD8 (53-6.7, Cy7PE conjugate), B220 (RA3-6B2), Mac1 (M1/70, APC conjugate), and Gr1 (RB6-8C5) (all from eBioscience, San Diego, CA). Data were collected using a multiparameter BD LSR II flow cytometer (BD Biosciences, San Jose, CA) and analyzed offline using FlowJo software (Treestar, Inc, Ashland, OR).

Preparation of dermal regenerative templates and parabiotic model.

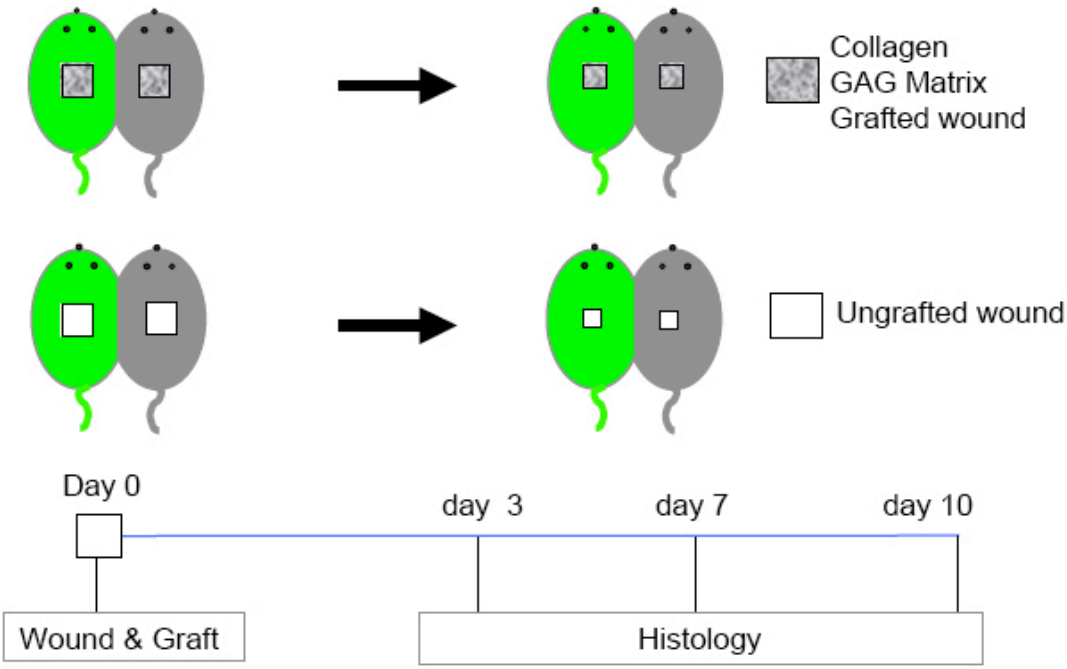

Figure 3. Parabiotic model used to study the contribution of circulating cells to wound regeneration (grafted wounds) and spontaneous healing (ungrafted wounds).

Acellular, ultrathin (0.5 mm), custom made collagen-GAG matrices were prepared at the Massachssetts Institute of Technology (MIT) as previously described.[6, 7] Scaffolds were grafted in the wounds and sutured to the wound edges with 6/0 nylon sutures.

Allogenic acellular dermal matrix was prepared from dermis procured from C57 Black mice using methods similar to those for making commercially-available micronized dermal matrix.[135] Briefly, the hair was removed from the dermis, the epidermis was removed, and the dermal matrix was decellularized using a combination of ionic and detergent solutions. The resulting acellular matrix was freeze-dried and subsequently cryofractured to produce micronized particles of

extracellular matrix between 100 and 200µm diameter. 187mg of this material was rehydrated in 500µl of a biochemically-stabilized platelet suspension and freeze-dried. The ratio of matrix to hydrating solution generated a final volume 2-times the volume of the diluent and was based on the ability of the final material to maintain its integrity, mold to non-uniform shapes, and produce a consistent dry cake following freeze-drying.

Collection of the platelets.

In order to generate lyophilized platelet concentrates, transfusion-quality human PRP was purchased from an American Association of Blood Banks accredited blood bank and used within 5 days of donation.[136] Freeze-dried PRP was prepared by combining PRP with a buffered biochemical stabilization solution and freeze-drying in a LyoStar freeze-dryer (FTS Kinetics Systems, Stone Ridge, NY), as previously described.[137]

At the Oklahoma Blood Institute, Oklahoma City, OK, PLTs were collected from the human blood donor by plateletpheresis using the instrument manufactured by COBE Spectra, Gambro BCT, Lakewood, CO at a ratio of 10 vol of blood to 1 vol of ACD (Formula A). The volunteer donor met the requirements of the AABB and took no medication known to affect PLT function for 10 days before donation. The study was reviewed and approved by the Institutional Review Board for Human Research, Oklahoma Blood Institute, Oklahoma City, OK. Informed consent was obtained from the donor. The PLTs were leukoreduced with a total WBC count of 5×10^6, contained more than 4.0×10^{11} PLTs, and were stored in two 200- to 300-mL volumes of plasma in 1000-mL CLX plastic bags.

Liquid preservation at 22ºC.

PLTs collected and stored in 1000-mL CLX (tri-2-ethylhexyl trimellitate) plastic bags were stored in a shipping container that maintained the temperature at room temperature during transportation by air from Oklahoma to Boston on the day of collection. Twenty-four hours after collection and transportation to Boston, the two 250-300 ml volumes were pooled and divided into three equal volumes. One volume was stored at room temperature at 22 C (room temperature) on an Eberbach shaker for 24 hours prior to testing.

Preparation of pGlcNAc patch and scaffold.

The microalgal-derived nanofibers that constitute the pGlcNAc (NAG) patch are produced by Marine Polymer Technologies, Inc., by a proprietary cGMP process. Briefly, microalgae are cultured in unique bioreactor conditions using a defined growth media. Following the harvest of microalgae from high-density cultures, nanofibers are isolated via a stepwise separation and purification process resulting in batches of pure nanofibers suspended in water for injections (wfi). Fibers are formulated into patches by concentration and oven drying, and are packaged and sterilized by gamma-irradiation. Nanofiber dimensions average 20-50nm x 1-2nm x ~ 100μm. Batches of fibers are individually quality controlled using chemical and physical test parameters, and each batch must meet strict purity criteria prior to release. Final batches are required to be substantially free of proteins, metal ions, and other components.

Protocol for NAG scaffold preparation.

In order to generate porous scaffolds of NAG fibers with regenerative properties, cultures of microalgae were processed through a series of freeze-drying cycles as for the preparation of the collagen-GAG scaffolds. Porosity of the scaffolds was measured by electron microscopy.Materials:

1. 500 mg 70% DEAC (short form of fibers MW $1X10^4$)
2. 110 mg 70% DEAC (long form of fibers MW $1X10^6$)
3. 60 mg short p-GlcNAc fibers

Preparation:

DEAC samples 1&2 in lyophilized form were dissolved in de-ionized water 10 ml each and mixed together in the glass container. Eight ml of sterile short fibers suspension 7.5 mg/ml was added to the mixture. Total volume of the sample was adjusted to 50 ml with de-ionized water. To achieve uniform solution mixture was sonicated 3min with 30W. 25 ml of the mixture were placed in the square plastic dish 9.5X9.5 cm^2 and lyophilized with regular protocol. After drying material was slightly compressed and cut in 36 small squares about 2 cm^2 each with total weight of polymer 3.7 mg/cm^2

Rat Ear Stretch Model.

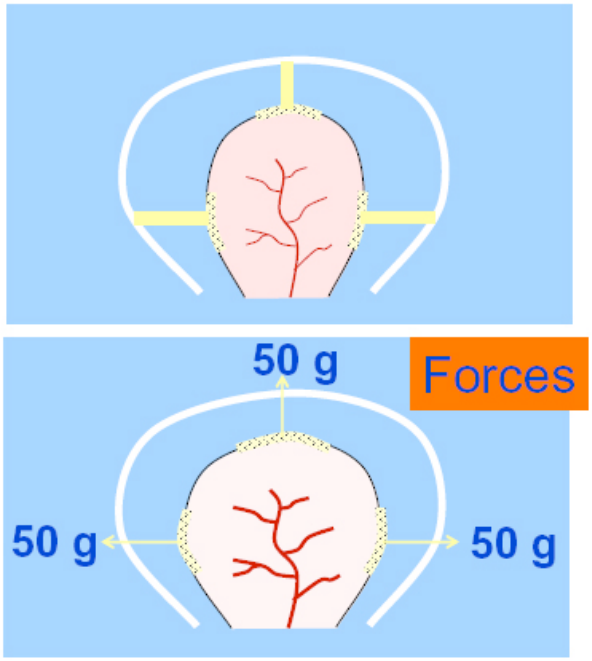

Figure 4. Rat ear stretch model. A custom made device was attached to rat ears to apply defined regimens of forces to a perfused tissue.

Wistar Rats (Charles River Laboratory) were cared for in an AAALAC certified facility under an approved experimental protocol. Ears were shaved 24-48 hours prior to the start of each experiment and attached to custom-built ring-shaped devices through three latex adhesive pads using cyanoacrylate glue (Dermabond®, Ethicon, Sommerville, NJ) and rubber bands. The rubber bands were calibrated for tension vs. distance stretched using a digital force gauge (DFI 10: Chantillon, San Leandro, CA). Continuous tension, 0.50 Newtons (approximately 50 g force) was applied for a period of 2 days, and 4 days continuously, or 8 hours cyclically - 2 hours on and 1 hour off. The ears of the tension-free animals received sham devices, with rubber bands free of tension. Each animal received a stretch device on one side and a sham device contralaterally.

Intravital Microscopy.

Intravital microscopy (IVM) pictures of the rat ear vessels were taken daily to monitor changes in vessel size and morphology. The main dorsal blood vessel along the y-axis of the ear was identified macroscopically. Areas of interest were marked using India ink prior to stimulating the ears. Serial images of the vasculature were taken of these pre-designated areas. Blood vessels in ears stretched for 4 days continuously and 8 hours cyclically were compared to the sham counterparts. Three groups of animals were included in the study: 2- and 4-day continuous stretch and 8-hour cylical stretch,

15 animals/group were studied. During stimulation, rat ears were viewed under a light microscope at 10X magnification at a fixed distance below the microscope lens. The ears were trans-illuminated from below using a light source of constant intensity. Digital images of the ear vasculature were taken from three different areas using a Kodak DC120 Digital Camera, (Kodak, Rochester NY). Vessel diameters were measured digitally using Adobe Photoshop® (Adobe, San Jose, CA).

Mercox™ Corrosion Casting.

72 hours after 2 or 4 days of continuous stretch or 8 hours of cyclical stretch, animals (n=3-6 animals per group) were euthanized for corrosion casting.

Mercox™ Embedding Resin Kits were obtained from SPI Supplies (West Chester, PA). Intravascular access, using an olive-tipped metal cannula, was established via the left ventricle while the rat was under deep anesthesia. After the descending aorta was suture ligated, a vent was created in the right atrium. The entire vasculature was subsequently irrigated with NS until clear of blood. Once the blood had been washed out, the vessels were perfusion fixed by flushing with 15 cc of a 2.5% glutaraldehyde solution. Subsequently, 15-20 cc of a Mercox/methyl-methacrylate/catalyst mixture was injected through the cannula to completely fill the ear vasculature and allowed to set. Ears were then carefully harvested, frozen in distilled water until time of processing. The tissue encasing the Mercox™ resin was corroded by boiling the ears in water (38^{o}C) followed by potassium hydroxide. The resulting vessel cast was then sputter coated using gold dust and viewed at 10 kV using a scanning electron microscope.

The VAC model.

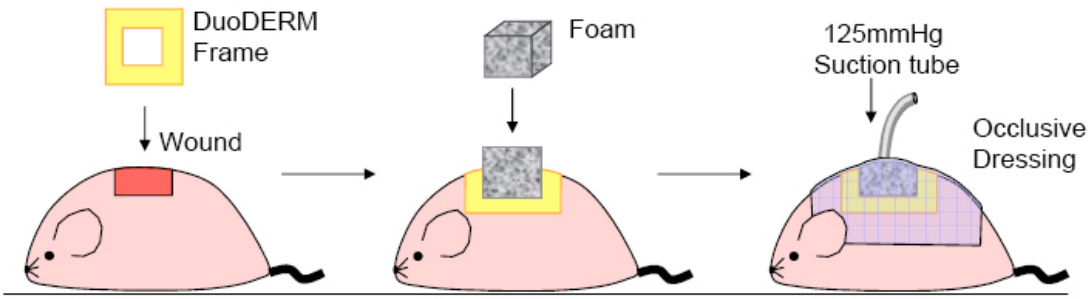

Figure 5. Schematic representation of the VAC model.

The VAC system (foam, semi-occlusive dressing and suction at 125 mmHg, V.A.C.®, KCI, San Antonio, TX) was compared with a semi-occlusive adhesive covering alone (KCI drape, San Antonio, TX). The VAC device resembled the clinically used continuous suction of 125 mmHg[138] (Fig. 5).

Microscopic Analysis.

Central wound cross-sections (n=10 per group) were embedded in paraffin, sectioned and stained according to routine Hematoxylin and Eosin (H&E) protocols. Panoramic cross-sectional digital images of each wound were prepared using Adobe Photoshop CS Software (Adobe Systems Incorporated, San Jose, CA).

These sections were analysed with digital planimetry (Image J, NIH, Bethesda, MD) by two independent treatment-blinded observers, to quantify the wound tissue. Granulation tissue in plasma treated wounds was arbitrarily set to 100%.

Immunohistochemistry.

Paraffin-embedded sections (n=10 per group) were re-hydrated and antigen was retrieved for Ki-67 analysis by microwaving in 10 mM sodium citrate (pH 6.0) for 10 minutes. Sections for platelet endothelial cell adhesion molecule-1 (PECAM-1) were treated with 40μg/ml proteinase K (Roche Diagnostics Corp.) for 25 minutes at 37°C. PECAM-1, (Pharmingen, San Jose, CA) and Ki-67 (Dako Corp., Carpinteria, CA) primary antibodies were incubated at 4°C overnight. PECAM-1, and Ki-67 signals were intensified using the tyramide amplification system (Perkinelmer, Boston, MA).

In PECAM-1 stained slides, the total number of blood vessels (positive for PECAM-1) was counted using 40x magnification.

In Ki-67 stained slides, the ratio of proliferating nuclei (positive for Ki-67) over total nuclei was quantified using 40x magnification.

10 microscopic fields at 40x magnification were used in each treatment arm and immunolocalization condition.

Ear samples (n=3), collected 72 hours after force application were bisected along the longitudinal axes and fixed in 10% neutral buffered formalin. Paraffin-embedded sections were re-hydrated and antigen retrieval for proliferating cell nuclear antigen (PCNA) analysis was accomplished by microwaving in 10mM sodium citrate (pH 6.0) for ten minutes. Sections for endothelial cell marker platelet endothelial cell

adhesion molecule 1 (PECAM-1) were treated as previously described and PCNA (Dako Corp., Carpinteria, CA) primary antibodies were incubated at 4°C overnight. PCNA staining was performed using Vectastain ABC Kit (Vector Laboratories, Burlingame, CA).

Wound Watch Staging System: Quantification of Vascular Area and Cell Proliferation.

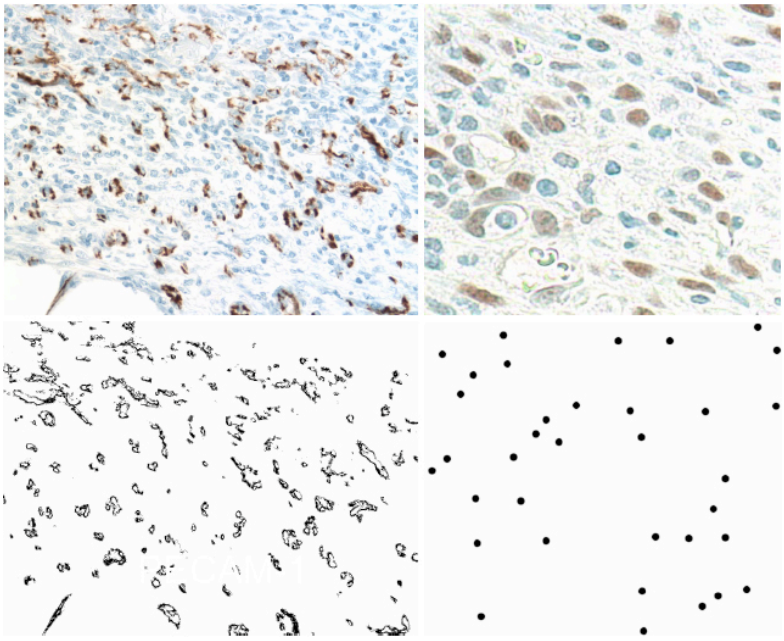

Figure 6. Immunolocalization of PECAM1 (top, left) and Ki67 (top, right) and digital analysis of the relative vasculature and cell proliferation as assessed in the wound watch staging system.

High power images of stained sections were used to quantify the degree of proliferation and vascularization and to compare treatments to spontaneous healing. Three digital images of PECAM-1 and Ki-67 stained slides were captured for each sample, one in the middle and two on the edges of the wound bed. Pictures were viewed with Adobe Photoshop CS Software, and blood vessels and proliferating nuclei in each high-powered field were marked and counted. Proliferating cells were counted as a ratio of proliferating nuclei (Ki-67-positive) to total nuclei.

Ratios were calculated between results obtained from the centre of the lesions and from the edges of each treatment group to the plasma treated group.

15 microscopic fields at 40x magnification were used in each treatment arm.

Finite Element Analysis of Rat Ear Stretch and VAC device.

The rat ear subjected to the stretch device was modeled using FEMLAB 3.1 (Comsol, Paris, France) software. The experiment was modeled as a 3D, structural mechanics, solid (stress and strain) representation with static analysis. The rat ear was modeled as

a linear, homogenous, elasto-plastic material and a number of specific mechanical properties were used. A Young's Modulus of Elasticity (E) of $2 \times 10^7 \frac{N}{m^2}$,[139] which is the approximate modulus of elasticity for human skin, was used, and a Poisson's Ratio (measure of the tendency of a stretched material to get thinner) (_) of 0.49 was assigned.[132]

The system was designed with the average dimensions of a rat ear (2.0cm x 1.6cm x 0.1cm). The three adhesive pads (used to apply tension) were then added and a composite object was created. Boundary conditions were implemented at A (left lateral pad), B (top pad), C (right lateral pad) and D (base of the ear). In accordance with the experiment outline, boundary A was given a force of –0.5 N in the x-direction, boundary B was given a force of +0.5 N in the y-direction and boundary C was given a force of +0.5 N in the x-direction. Boundary D is where the rat ear is attached to the body and therefore was constrained in the x, y and z directions. The model was then meshed, refined and solved. Results were expressed in kPA (1.0 kPA = 1000 N/m^2).

The VAC group was modelled by imposing a 125 mmHg upward suction within the foam pores an equal and opposite downward compressive force on the foam struts. For the purpose of the model we assumed the pore diameter to be 1.2 mm and the space between pores to be 1 mm. The outer boundaries of the soft tissue were left unconstrained and the pores as well as struts were constrained in the x and y directions allowing for the resulting stresses and displacements to be seen solely in the z direction.

Statistics.

All statistics and graphs were calculated and plotted using Sigma Plot Software (Systat Software, Inc.; Point Richmond, CA). One-way analysis of variance and ad hoc LSD tests were used to determine the differences between experimental groups. Multivariate analysis was performed using Statistica v7.0 (StatSoft, Inc, Tulsa, OK). A p-value of 0.05 was considered significant.

In each rat the ratio stretch/sham was calculated. A paired student's t-test was used to determine statistical significance. A p-value of 0.05 was considered statistically significant.

4. Results

Wound healing kinetics in db/db and db/+ (wild type) animals.

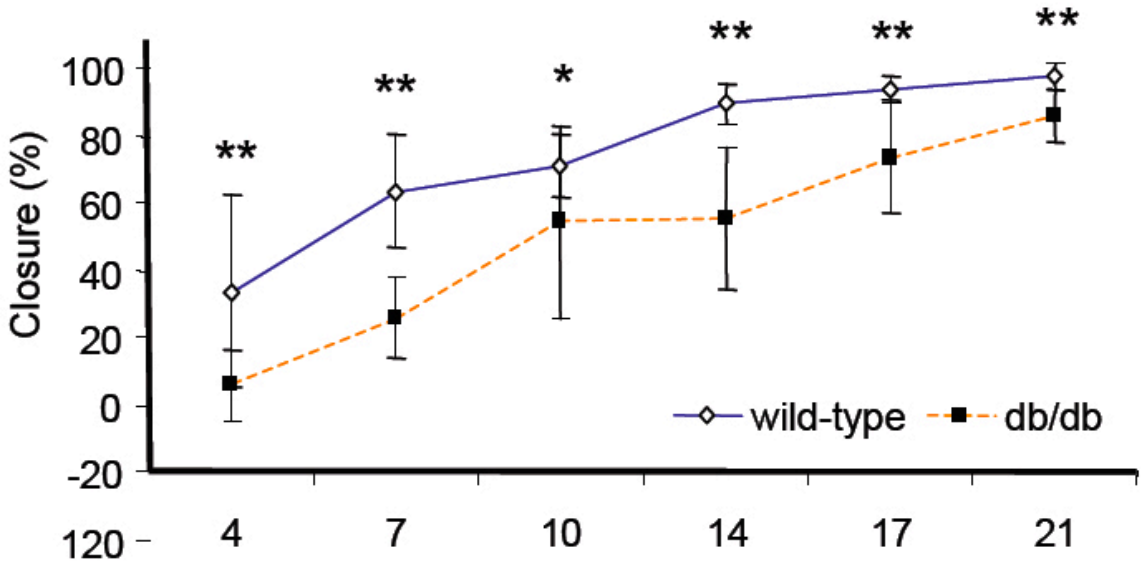

Figure 1. Wound closure kinetics in wild-type and diabetic animals. **=p<0.005; *=p<0.05.

Wound closure kinetics of full thickness wounds were followed up throughout the 21-day study (Fig. 1) and macroscopic pictures of wounds were quantified twice a week. On all days of the follow-up period, there was a marked increase in closure by wt animals compared to db/db animals ($p<0.005$ days 4, 7, 14, 17, 21; $p<0.05$ day 10) (Fig. 1). Approximately 50% wound closure was achieved on day 10 in db/db mice, 4.5 days later than in wt mice ($p<0.05$) (Fig. 1). Between days 10 and 21, db/db mice continued to reduce their raw surface area, but only achieved 86 ± 8% closure by day 21, whereas wild-type mice were 90% closed by day 15 ($p<0.005$) (Fig. 1).

Development of the parabiotic model.

4-week old animals were joined in parabiosis before the clinical onset of diabetes-related wound healing complications. Under such conditions and as in previous studies,[54] all diabetic animals (db) developed the full diabetic phenotype while in the parabiotic condition regardless of their partners (db or wt). Chimeric and control pairs were rested 4 weeks after parabiosis surgery to allow for complete healing of the

parabiotic joining wound and for the establishment of peripheral blood cross-circulation.

To verify the development of cross-circulation between animals in each parabiotic condition, we examined the distribution of an intravascular dye (Evan's blue) across the joining wounds. After injection into one animal of the pair, the Evan's blue dye immediately flushed the same animal and progressively spread through the common vascular tree at the junction to its partner, as demonstrated by progressive skin discoloration (Fig.2a,b). Spectrometry of serum samples collected from each animal 120 minutes post injection demonstrated full equilibration of the dye in the serum of both db::wt chimeras and wt::wt wild type control pairs, although in diabetic db::db control pairs dye concentration in the uninjected partner was only ~50% the level in the injected animal at this timepoint (Fig.2c).

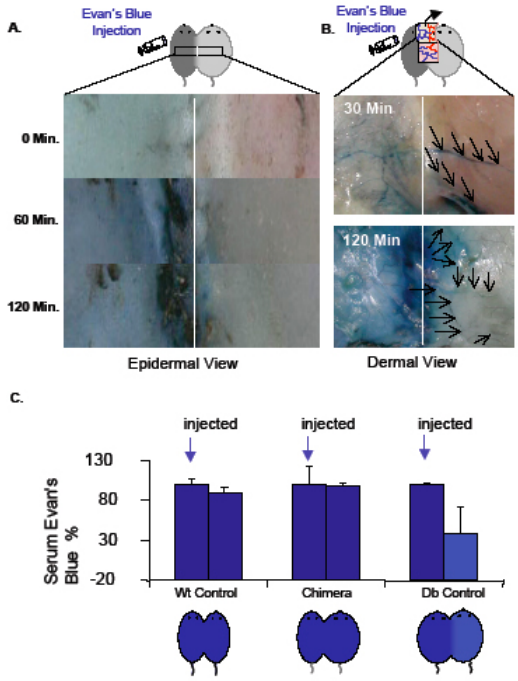

Figure 2. Evan's blue injection demonstrates the presence of cross circulation between the two animals.

Previous studies from the parabiotic model developed by Coleman showed that the cross-circulation of high levels of leptin from diabetic to wild type partners may cause changes in food intake by wild type parabionts[1-3]. In contrast, in our model, biopsies from the gastro-intestinal system of chimeric pairs (wt::db) harvested at necropsy revealed normotrophic organs in both partners, a sign of regular feeding (data not shown). In general, animals in each group tended to lose ~30% of their initial body

weight in the first week after the parabiosis operation. Although in diabetic chimeras, cholesterol levels in the db partner were lower, and leptin levels higher, compared to db controls, there were no differences in absolute weight loss between the different experimental groups, and the weight of all animals stabilized before the start of the dorsal wound healing study (data not shown).

Exposure to a normal systemic environment improves wound healing in db parabionts. To study the role of circulating factors in diabetic wound healing, both animals in chimeric and control parabiotic pairs received a full thickness dorsal skin injury.

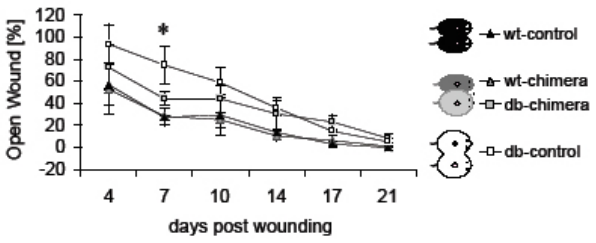

Figure 3. Wound closure in db-chimera is improved compared to db-control on day 7. *=p<0.01.

Quantification of wound closure across study groups confirmed that wound healing was delayed in db animals; however, strikingly, these studies also revealed that the rate of wound healing in db animals was significantly enhanced by parabiosis to a wild type partner, as compared to wound healing in diabetic control pairs (db::db). This effect was significant at day 7 after wounding, when control diabetic animals joined to diabetic partners still showed ~75 +/- 16% open wound area (defined as wound surface not covered by epithelium[137]), while db animals joined to wild type partners showed a significantly smaller (44% +/- 6%, p<0.01) open wound (Fig. 3). These data appear to reflect a beneficial impact of exposure to wild type circulation on the rate of diabetic wound healing. Interestingly, exposure to circulating factors from diabetic mice did not alter wound closure in wild type animals of chimeric pairs (db::wt) when compared to wild type control pairs (wt::wt). Toward the end of the follow-up, the natural tendency of diabetic animals to heal spontaneously by contraction[140] obscured the parabiosis-induced differences noted on day 7. In light of these data indicating that macroscopic differences in wound closure capacity were most apparent at day 7 after wounding, we focused principally on this time point for additional analysis of the parabiotic effects related to diabetic wound healing.

Fully healed wounds in diabetic partners of wild type mice show increased collagen deposition.

At 3 weeks after injury, wounds on chimeric and control parabionts showed no macroscopic differences, and all animals exhibited near complete wound closure

(Fig.3). However, significant differences still remained in wound histology, even among fully closed wounds.

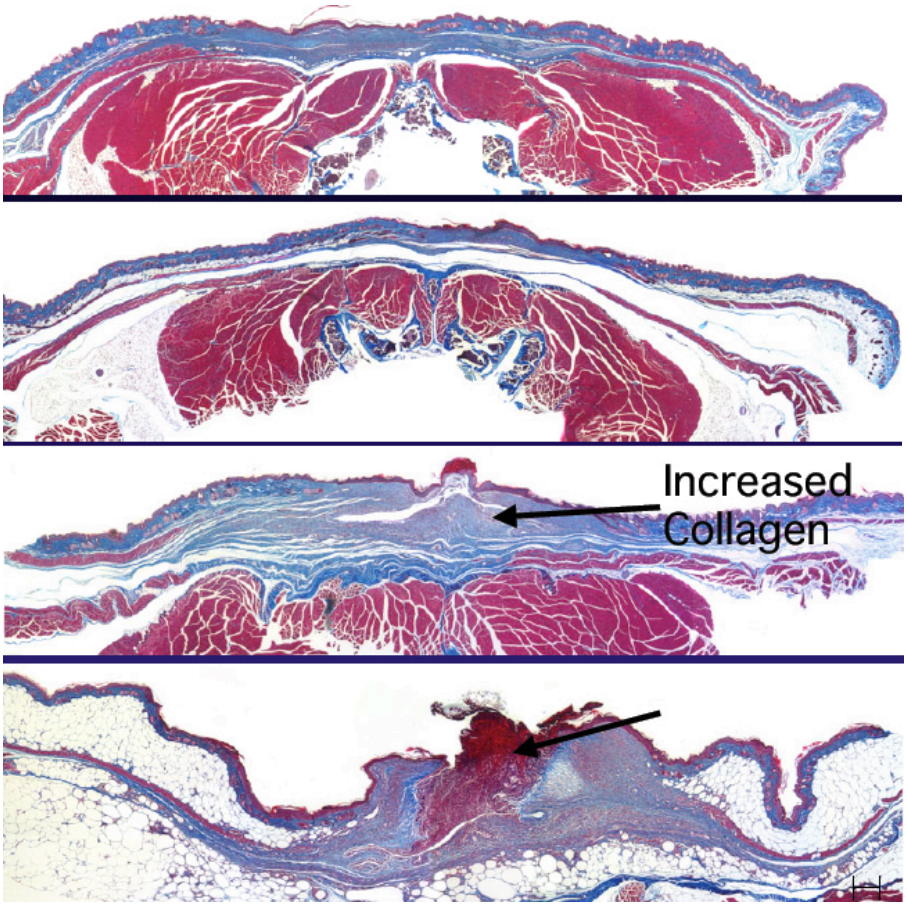

Figure 4. On day 21, collagen deposition is increased in db-chimera compared to db control.

In wild-type animals, wounds were filled with collagen - characterizing the newly formed extracellular matrix - regardless of their parabiotic partner (wt::db and wt::wt) (Fig. 4). In contrast, wounds on diabetic controls (db::db) showed scant collagen deposition and immature organization (Figure 4).

Glycemia and Leukocyte Presence. To understand whether parabiosis to a healthy animal affected primarily diabetic metabolism or contributed mainly by modulating circulating cells, we evaluated glycemia as main metabolic parameter in diabetes and analyzed circulating leukocyte subsets to monitor inflammatory cells in control and chimeric parabionts. Surprisingly, improved wound healing in diabetic partners of wild type animals was not associated with normalization of blood glucose levels. Peripheral blood glucose levels in diabetic animals were consistently hyperglycemic (>550 mg/dl) throughout the study, whether these mice were joined in parabiosis with wild type or diabetic partners (Figure 8A). Similarly, wild type animals, regardless of their partners, showed significantly lower blood glucose levels (100 - 130 mg/dl) than

diabetic animals (Figure 5, $p<0.01$). As rapid cross-circulation clearly exists diabetic chimeras (Figure 5), these results likely reflect rapid metabolism of excess blood glucose within the wt partner.

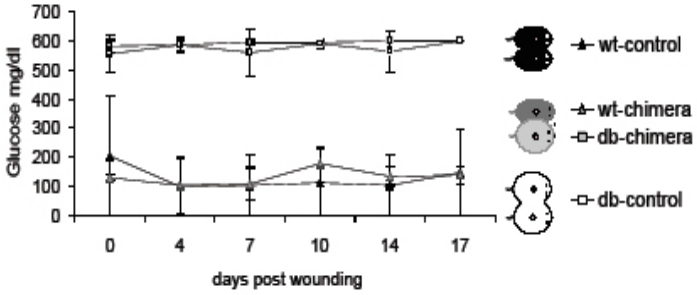

Figure 5. diabetic animals remained hyperglycemic regardless from their parabiotic partner.

On day 7 after injury, the frequency of different leukocyte subsets and the degree of inflammatory infiltrate in wounds were determined for each experimental group by flow cytometry and histological analysis, respectively. Flow cytometric analysis revealed higher levels of circulating neutrophils in diabetic control parabionts as compared to wild type controls. Notably, neutrophil frequencies were significantly decreased in diabetic mice when connected to a wild type partner (Fig. 6a, $p<0.05$). No significant differences were detected in circulating levels of monocytes or T cells (Fig. 6b) In contrast, circulating B-cells in diabetic animals were increased (Fig. 6b, $p<0.05$) in chimeric pairs, as compared to diabetic animals in control pairs (db::wt).

Interestingly, immunohistological staining of wound tissues on day 7 with the pan-hematopoietic marker CD45 demonstrated that wounds of diabetic mice in chimeric pairs (db::wt) exhibited a significantly greater (~4-fold, $p<0.01$) inflammatory cell infiltration when compared to diabetic control wounds (db::db). In fact, this level of inflammatory infiltrate was equivalent to that seen in wild type animals (db:wt and wt::wt) (Fig. 6c,d). Importantly, this normalized inflammatory response likely involved improved recruitment or enhanced local proliferation of both wt and db hematopoietic cells, as indicated by the fact that wounds on db::wt pairs in which the wt partner was marked by GFP expression showed that only 20% of the CD45+ or CD11b+ cells in the wound bed derived from the wt animal.

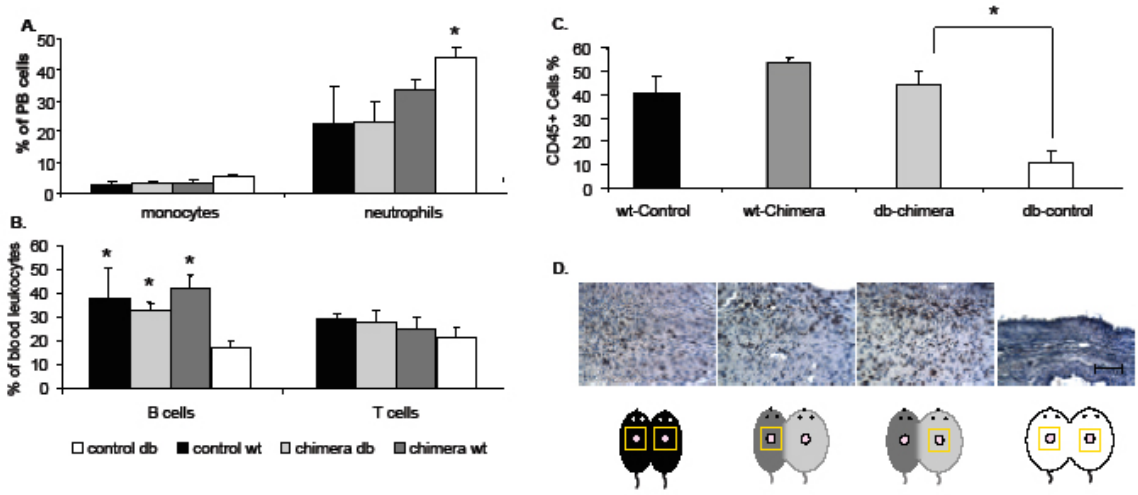

Figure 6. Modulation of circulating and engrafted leukocytes due to parabiotic conditions. *=p<0.05.

Together, these data argue that normalization of circulating leukocyte subsets and improved recruitment, proliferation, and activity of inflammatory cells in the wound tissue is a major mechanism by which parabiosis to a wt partner improves diabetic wound repair.

Tension application system and predicted responses

For studying the effects of tension on perfused systems, we developed a new *in vivo* rat ear model. The ear, being thin and semitransparent, allowed for the quantification of the response of the blood vessels to forces using in vivo microscopy (IVM) over time, without harvesting the tissues.

We first modeled the effects of force application on the rat ear to assist in the design of our tissue analysis. To determine the expected distribution of stresses throughout the ear tissues in response to applied tension, Von Mises stress plots were constructed from the solved finite element equations (Fig. 7a).

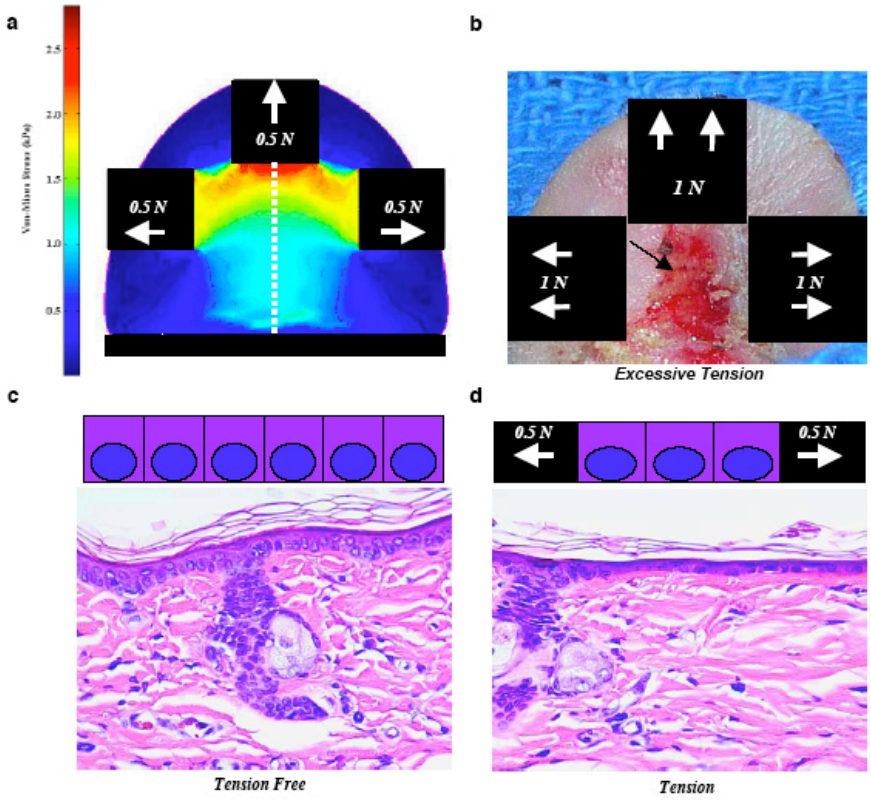

Figure 7. Tissues subjected to forces showed characteristic strains.

Although skin is generally considered to be a non-linear, viscoelastic material,[141] results from the Von Mises stress plot along the y-axis appeared linear until approximately 2 kPa of force (Fig. 7a); thus, the ears were modeled as linear materials. The Von Mises stress curve can be broken into two main linear ranges of approximately 0 to 1(low level) and 1 to 2 kPa (mid-level) of force, both extending approximately 2 mm into the tissue (Fig. 7a). A third range of 2 to 3 kPa (high level), extending approximately 1 mm closer to the apical adhesive pad was also identified. Preliminary studies using the tension application device showed that forces in the range of 1N (approximately 100 g, Fig. 7b) induced tissue injury within 4 hours of application, characterized by edema, oozing and bleeding through the damaged epithelium, de-epithelialization, and the appearance of extravasated cells in the interstitial space. When this type of injury is induced, the inflammatory response masks the effects of micromechanical forces. Thus, we chose to use a lower tensile load of 0.5 N, which elicited vascular changes without inflammatory response as confirmed with histological sections. Forces applied to the ears induced cell displacement, particularly in the epidermal layer, and straightening and realignment of collagen fibers in the dermal layer (Fig. 7c,d)

Tension application increases blood vessel diameter

In the mid-level (1-2 kPa) force region, analysis of the size of rat ear dorsal blood vessels using IVM revealed a progressive increase in the diameter of the main longitudinal vessel over time (Fig. 8a,b). The vessel increases in size by approximately 30% within 6-8 hours of cyclical forces ($p<0.01$), when compared to sham ears (Fig. 8a). When continuous tension was applied over days, progressive increases in diameter were observed, starting after 2 days, and resulting in more than a doubling of vessel diameter by 4 days ($p< 0.001$) (Fig. 8b,c), when compared to sham ears (Fig, 8b,d).

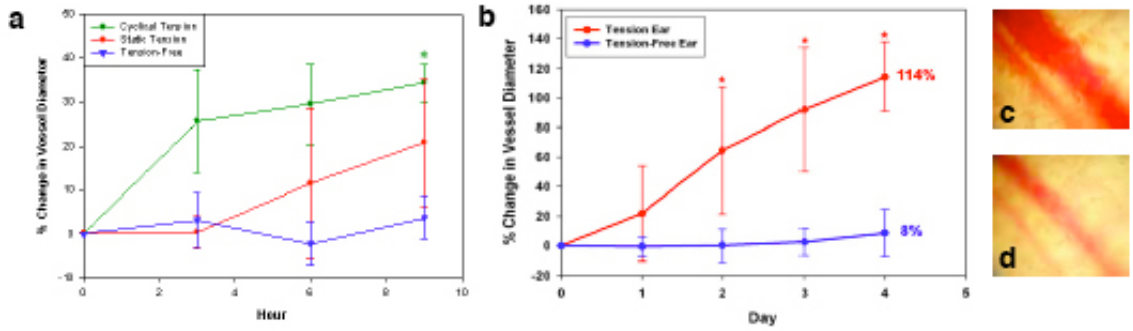

Figure 8. Increase in blood vessel diameter due to application of tensile forces. *=$p<0.01$.

We also made casts of the microcirculation to visualize the morphological changes in the vasculature subjected to forces. Overall, the microcirculatory network subjected to mid level forces displayed microvessels with a less homogeneous caliber and higher curvature (Fig. 9). Interestingly, microvessels subjected to forces showed the highly oriented tridimensional direction, as if forces redirected their distribution in the dermal space along the main force vector direction.

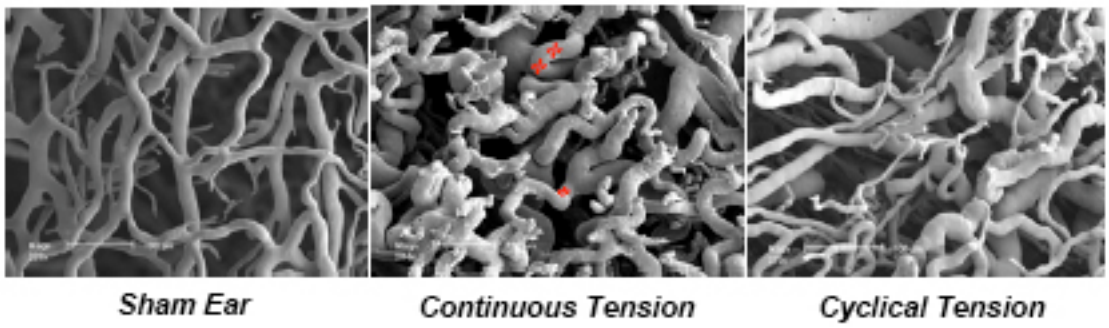

Figure 9. Vascular casts of the microcirculation show changes induced by tension to the microcirculation.

Heterogeneity in caliber of the vessels and increased curvature are early signs of vascular remodeling. These peculiar changes are characteristic of the casts collected after the application of continuous force, and cyclical stretch regimens were also able to induce similar initial signs of vascular remodeling (Fig. 9).

Tension induced Cell proliferation.

In the epidermis, cyclical regimens of mid-level forces (1-2 kPa) increased cell proliferation by a factor of 1.8 ($p<0.05$) while in the area subjected to 1 kPa no changes were seen (Fig. 10a). When the same forces were applied continuously for 2 days, a 3-fold increase in epithelial proliferation was observed ($p<0.01$), with PCNA positive cells increasing from 13% to 39% (Fig. 10b) compared to sham ears. Cell proliferation levels induced by this mid-level force regimen were also higher ($p<0.05$) when compared to the proliferation rate of cells within regions subjected to the lower force regiment (0-1 kPa) (Fig. 10b). After 4 days of exposure to mid-level forces, a 2.8-fold increase in cell proliferation was observed ($p<0.01$) relative to controls (Fig. 10b-d), and the lower force level induced a 4-fold increase in cell growth ($p<0.01$) (Fig. 10b).

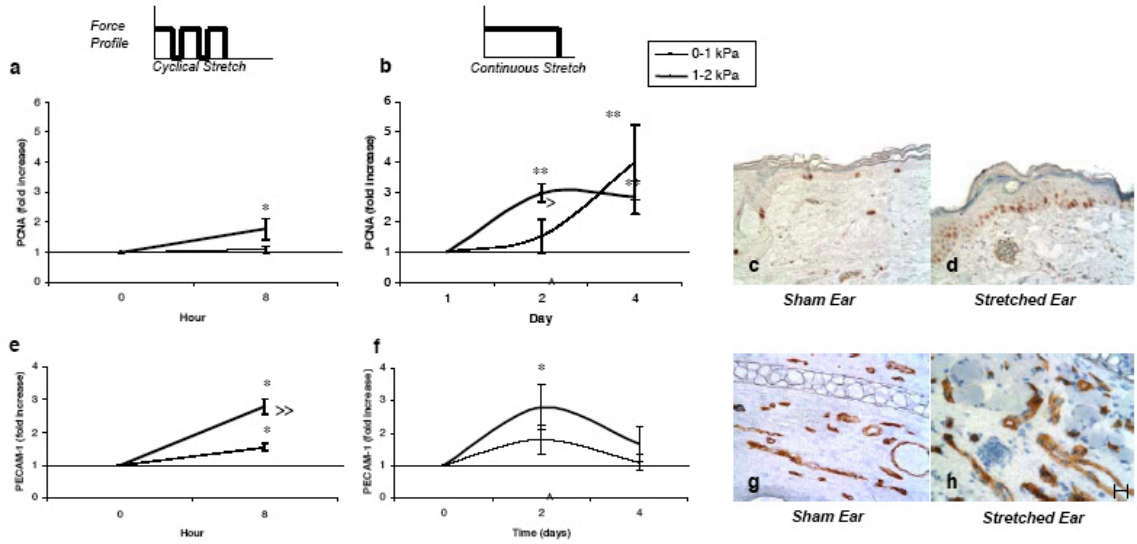

Figure 10. Increases in cell proliferation and vascular area induced by tension. **=p<0.01; *=p<0.05.

When fibroblasts and endothelial cell proliferation rates were quantified, no difference was seen between tension and tension free tissues.

After observing the characteristics of the physical data and trendline curves, an emphirical graph general model was generated to predict cell response to the application of forces using increased vascular remodeling and proliferation as markers of tissue function (Fig. 10). As shown, tissue growth is induced with the application of increasing
tension.

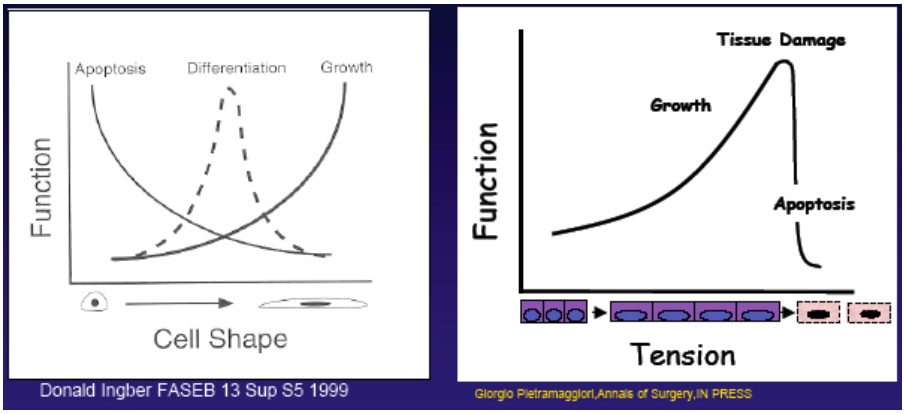

Figure 11. Theoretical response of cells and tissues to mechanical forces in vitro (left) and in vivo (right).

The curve depicting the tissue response to increasing amounts of force has a maximum slope illustrating the point at which maximal safe stimulation is achieved. After the maximal stimulation, tissue damage occurs, the tissue loses its physical properties, homeostasis is lost and cells lose their ability to respond to mechanical forces and undergo apoptosis, as previously shown in vitro.[95]

Wounds grafted with scaffolds.

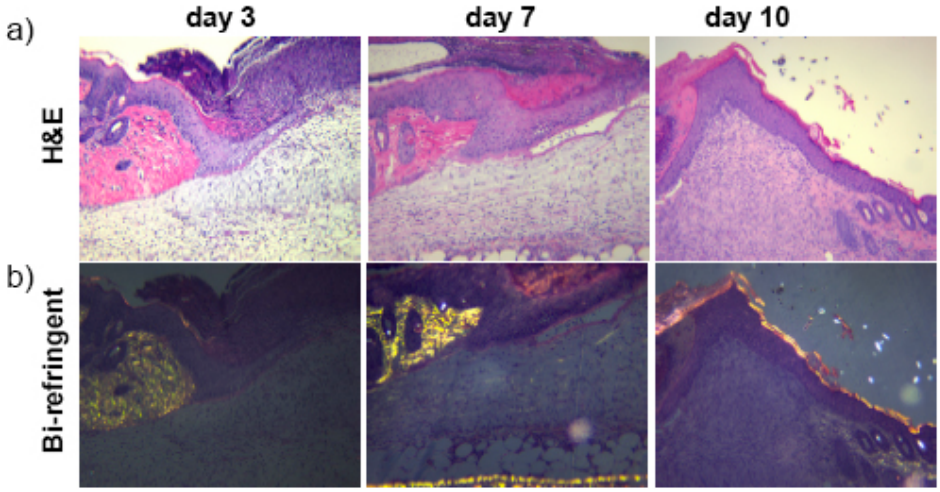

Figure 12. Integration of the collagen-gag scaffold into the healing wounds.

Spontaneous closure of skin wounds in rodents occurs mainly by contraction and secondarily by scar formation (due to the mobility of the skin). Collagen-GAG scaffolds, grafted on full-thickness wounds in mice, completely integrated into the healing tissues (Fig. 12). H&E stainings show epithelial cell from the uninjured wound edges sliding over the wound tissue grafted with Collagen-GAG Matrices (Fig. 12a). Bi-refringent microscopy shows the difference between the Collagen-GAG Matrix and the uninjured mouse skin, verifying the engraftment of the Collagen-GAG matrix (Fig. 12b). Bundles of uninjured dermis lighten up whereas decoiled collagen fibers of the Collagen GAG Matrix appear dark (Fig. 12b).

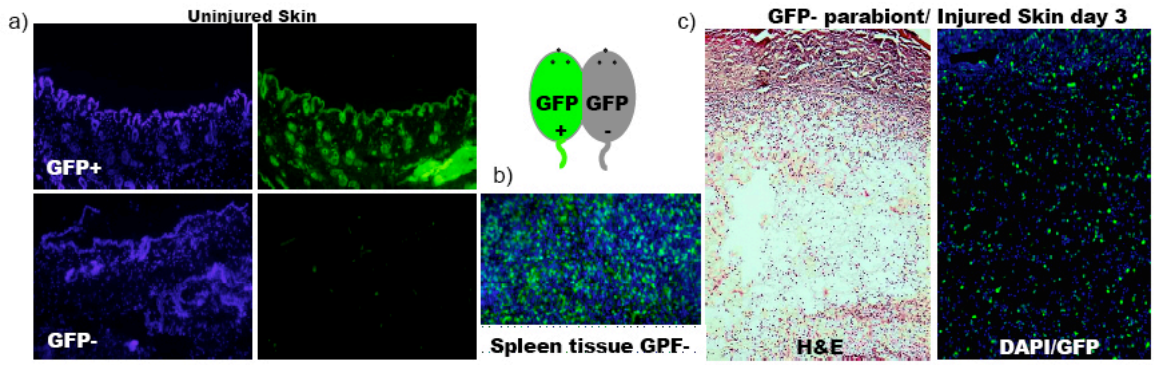

Figure 13. Circulating cells engraftment in uninjured and injured tissues.

In parabiotic animals in which an EGFP+ and an EGFP- animal were joined, circulating cell engraftment of EGFP positive cells into uninjured skin of the EGFP negative mouse was lower than 2% (Fig. 13a).
Spleen tissues of the EGFP negative mouse harvested 2 weeks after the parabiosis operation showed almost 50% chimerism (EGFP positive/negative, Fig. 13b).
Histological cross sections of injured skin from EGFP negative mice stained for H&E (left) and DAPI and GFP (right) showed engraftment of EGFP positive cells into the Collagen-GAG Matrix on day 3 (Fig. 13c).

Cells, circulating in peripheral blood, engrafted into the scaffolds and partecipated to the inflammatory infiltrate present into the scaffolds. Cross sections of wounds on EGFP negative mice were stained for DAPI and GFP on day 3, 7 and day 10 post wounding (Fig. 14a).
Quantification of EGFP positive cells in wounds on EGFP negative mice showed higher engraftment rates of circulating cells on day 3 when compared to day 10 (Fig. 14b). No difference in cell engraftment rates from the circulation on all days was noted between collagen-GAG matrix grafted wounds and ungrafted ones (Fig. 14b).

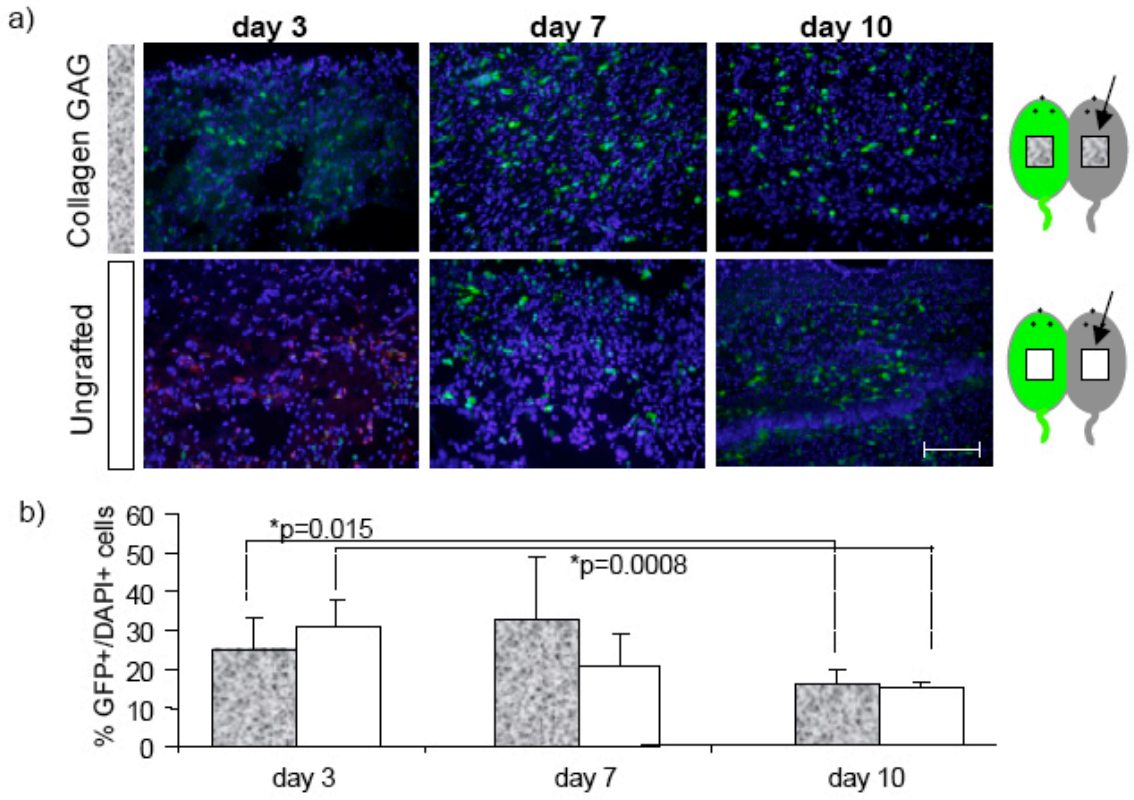

Figure 14. Circulating cell engraftment into wound tissues.

Signs of revascularization started to appear on day 7 and 10 into the scaffolds, while, control, ungrafted wounds, showed the earliest signs of angiogenesis on day 4.

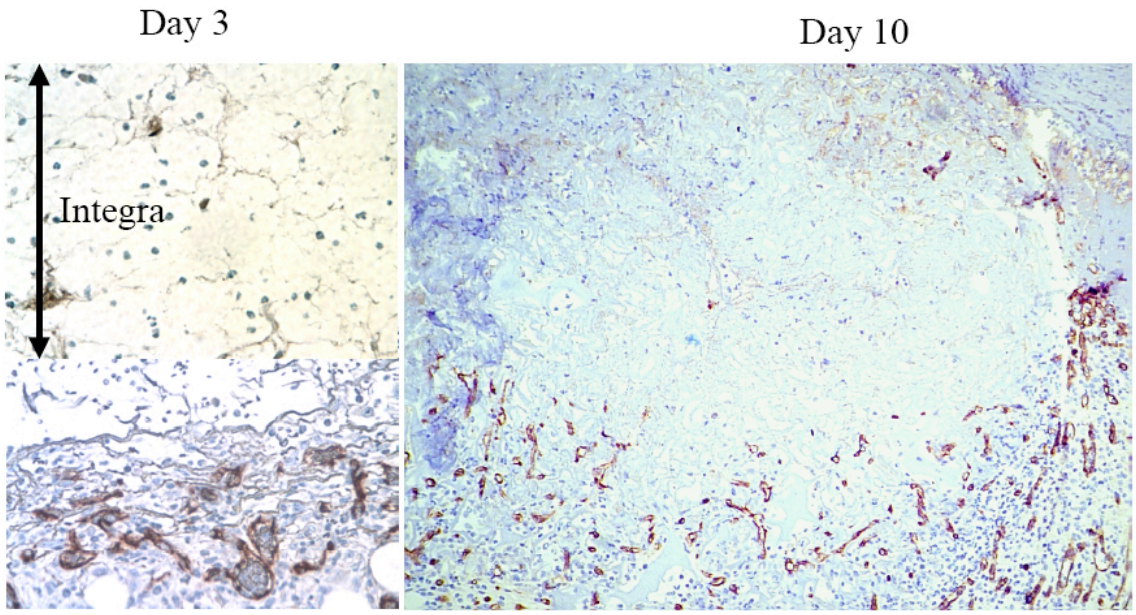

Figure 15. Limited revascularization of collagen-gag scaffolds (integra) during healing.

Circulating cells, populating the scaffolds were mainly CD45 positive (inflammatory cells, not shown), while absent was the contribution to endothelial cells from circulation (Fig. 16). From the histological sections it was also noticed how the scaffolds may have acted as physical barrier slowing blood vessel ingrowth (Fig. 15, 16)

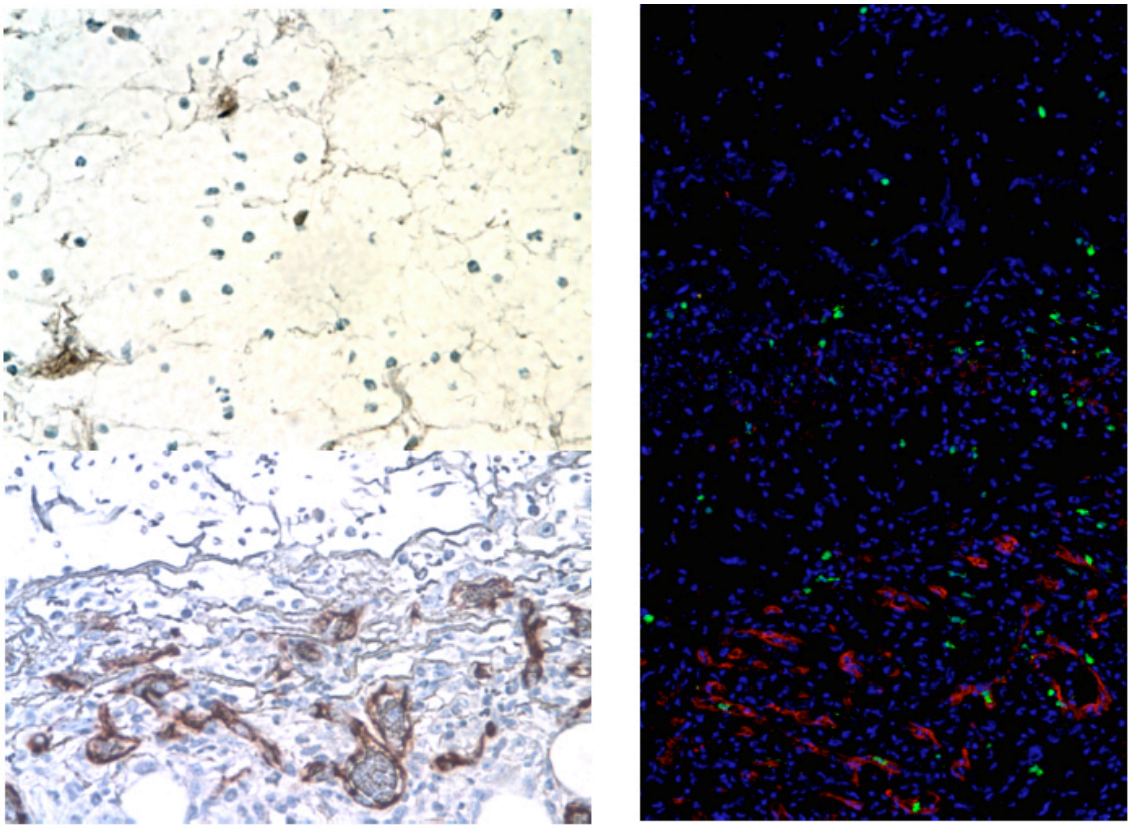

Figure 16. Absent contribution of circulating cells (in green, on the right) to collagen-gag scaffold revascularization (in red CD31 staining).

Wound strain induced by the VAC device.

We created a finite element model to predict the deformations and stress distributions on the wound surfaces treated with the VAC device or untreated controls. Mathematical modelling predicts no changes in stress induced by the control (occlusive dressing). Suction dressing produced a uniform increase in stress. The complete VAC showed high induction of stress on the wound microsurface that ranged from 1.5 to 2.5 kPa (Fig. 17). Tissue deformation is shown in histological cross-sections of each group. Wound bed strain was analysed in tissues fixed under different dressing modes *in situ*. Histological cross-sections of the wound bed were analysed for wound surface strain by dividing the difference between the

microdeformed surface length (l) and the linear length (l_0) to the linear length (l_0). The values are expressed in percentage (strain= (l- l_0)/ l_0 * 100). Foam struts in between vertical undulations caused local tissue compression (vertical arrow), whereas tissues between these areas are stretched laterally (horizontal double arrow).

Wounds treated with VAC dressing showed high levels of surface deformation ($p<0.005$) when compared to control wounds, with up to 60% strain on microscopic cross sections due to microdeformations ($p<0.05$, Fig. 17).

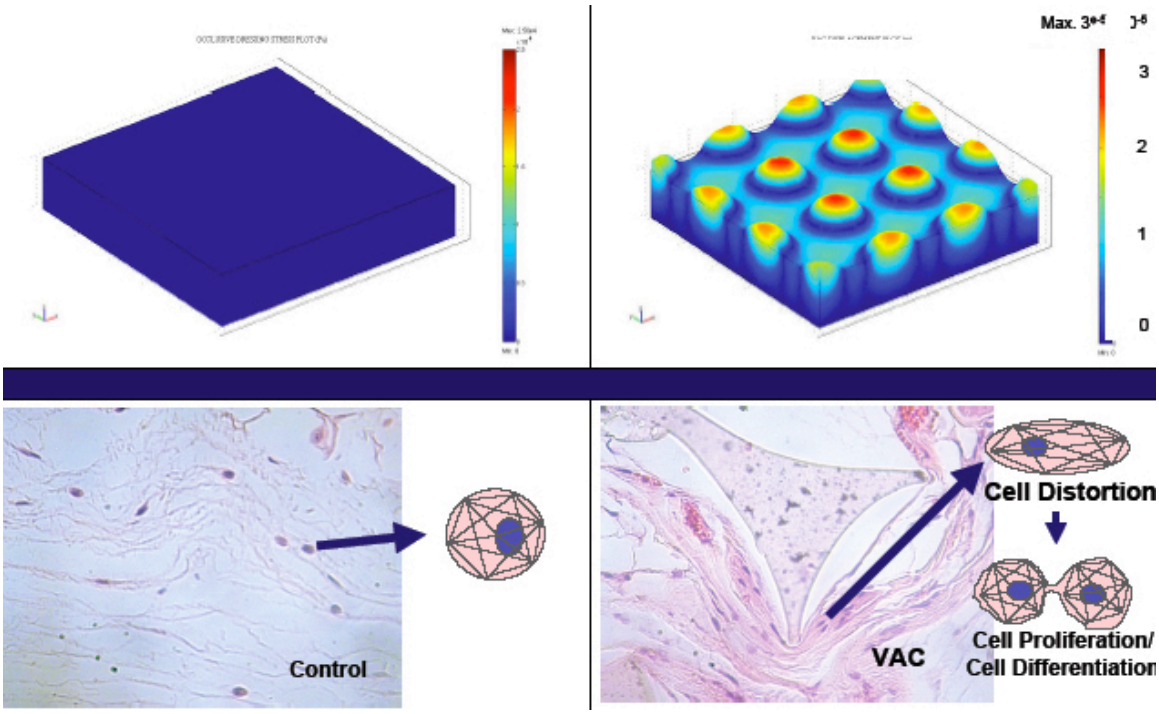

Figure 17. Wound bed strain analysis induced by the VAC device.

Wound Watch Staging System.

To stage wound healing, we adopted an innovative staging system based on histological immunolocalization of cell proliferation and vascularity. On day 7, the proliferation rate of cells populating the granulation tissue, was assessed by nuclear staining for Ki67 or PCNA, markers for actively replicating cells, and wound bed vascularization, was assessed using PECAM1, a pan-endothelial surface marker. Both factors are important during healing in order to generate new tissue.

Both signals were significantly enhanced in diabetic partners in chimeric parabiosis (db::wt), as compared to diabetic control wounds (Fig. 18a). Wound bed vascularity (quantified based on the area of PECAM-1 reactivity) was ~2-fold increased in diabetic chimeras compared to db::db control wounds ($p=0.05$) (Figure 18b) and was

similar to levels found in wounds of wild type animals of chimeric couples, although wild type control wounds (from wt::wt pairs) still showed higher ($p<0.01$) vascular area when compared to diabetic controls (Figure 18b). These data suggest that parabiosis to a wt partner increases the rate of angiogenesis at the wound site, a hypothesis that is further supported by the faster rate of blood exchange that we observed across the anastomosed vasculature of parabiotic chimeras, as opposed to diabetic control pairs. Similarly, the rate of cell proliferation of healing diabetic chimeras was increased 2.6-fold ($p<0.01$) when compared to control diabetic pairs (db::db) (Figure 18b).

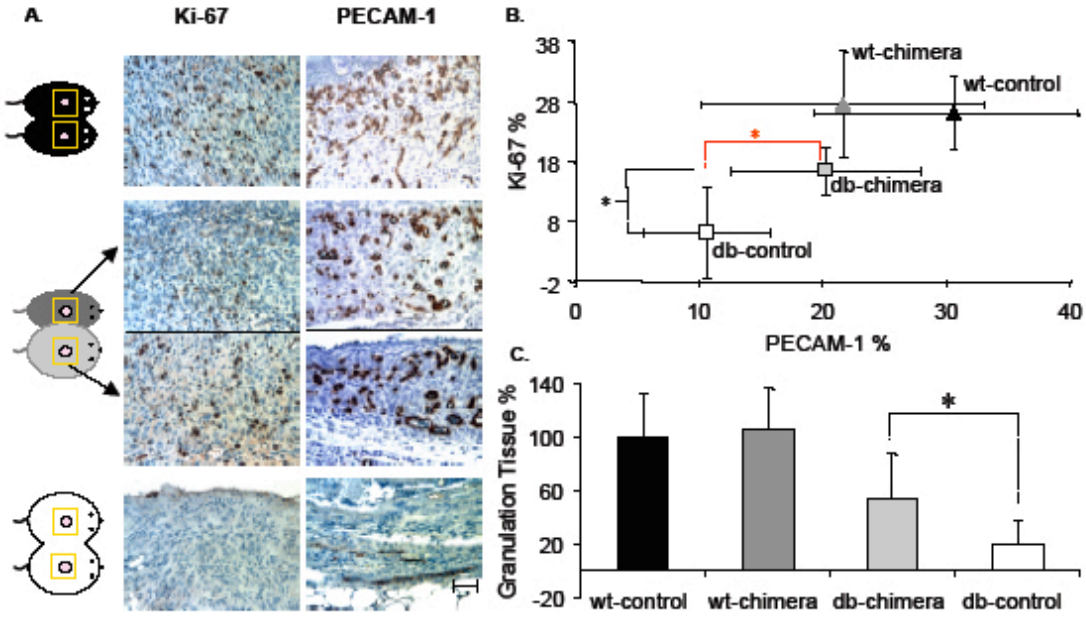

Figure 18. Increases in cell proliferation, vascularity and granulation tissue induced by chimeric conditions. *=$p<0.05$.

Wild type partners of chimeric pairs (wt::db) and wild type control pairs (wt::wt) showed significantly greater ($p<0.01$) cell proliferation as compared to diabetic control pairs, and a trend toward increased cell proliferation when compared to diabetic partners of chimeric pairs (db::wt) (Fig. 18b). Wounds treated with high doses of VEGF, the most potent angiogenic factor, showed 10.5 fold-increase ($p<0.01$) in vascularity compared to untreated controls (Fig. 19), while did not show

significant increases in cell proliferation and healed producing an immature collagenic bed (Fig. 19). PRP (combining growth factors and an efficient drug delivery system) stimulated both parameters with 2.8-fold increase ($p<0.01$) in vascularity and up to 4-fold increase ($p<0.01$) in cell proliferation when compared to untreated wounds (Fig. 19).

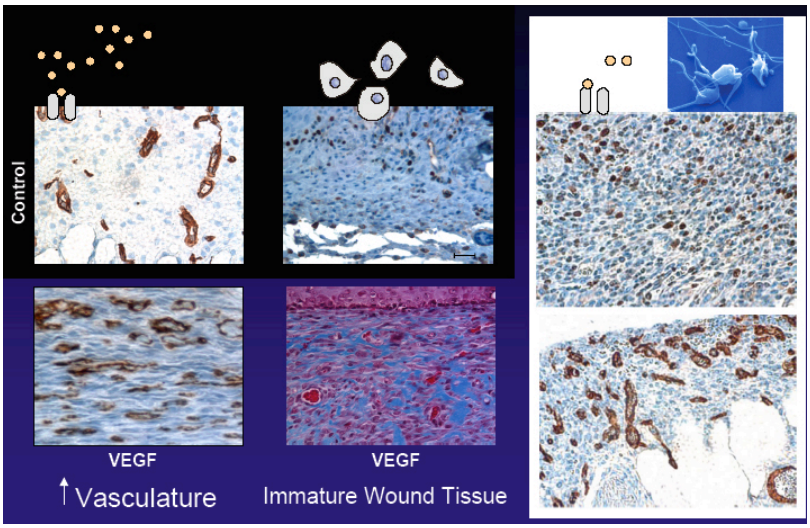

Figure 19. VEGF (left bottom), and PRP (white rectangle) are compared to untreated controls.

The stimulation of autologous, circulating platelets with the use of the NAG polymer, achieved comparable levels of stimulations to the ones observed after the use of PRP (Fig. 20).

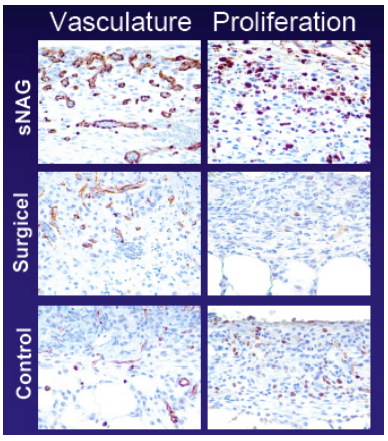

Figure 20. Stimulation of angiogenesis and cell proliferation induced by the NAG polymer compared to untreated wounds and chitosan based hemostatic controls.

The poly-N-acetylglucasamine polymer was also compared to another hemostatic agent (Surgicell), to prove its specific ability to stimulate healing (Fig. 20).

The two-dimensional quantification revealed that VAC treatment increased cell proliferation rates ($p<0.005$), with up to 4.7-fold increase in cell proliferation compared to control wounds (Fig. 21). When blood vessels were quantified, wounds

subjected to the VAC device showed a 2.2 - fold increase in blood vessel density when compared to the untreated ($p < 0.05$, Fig. 21).

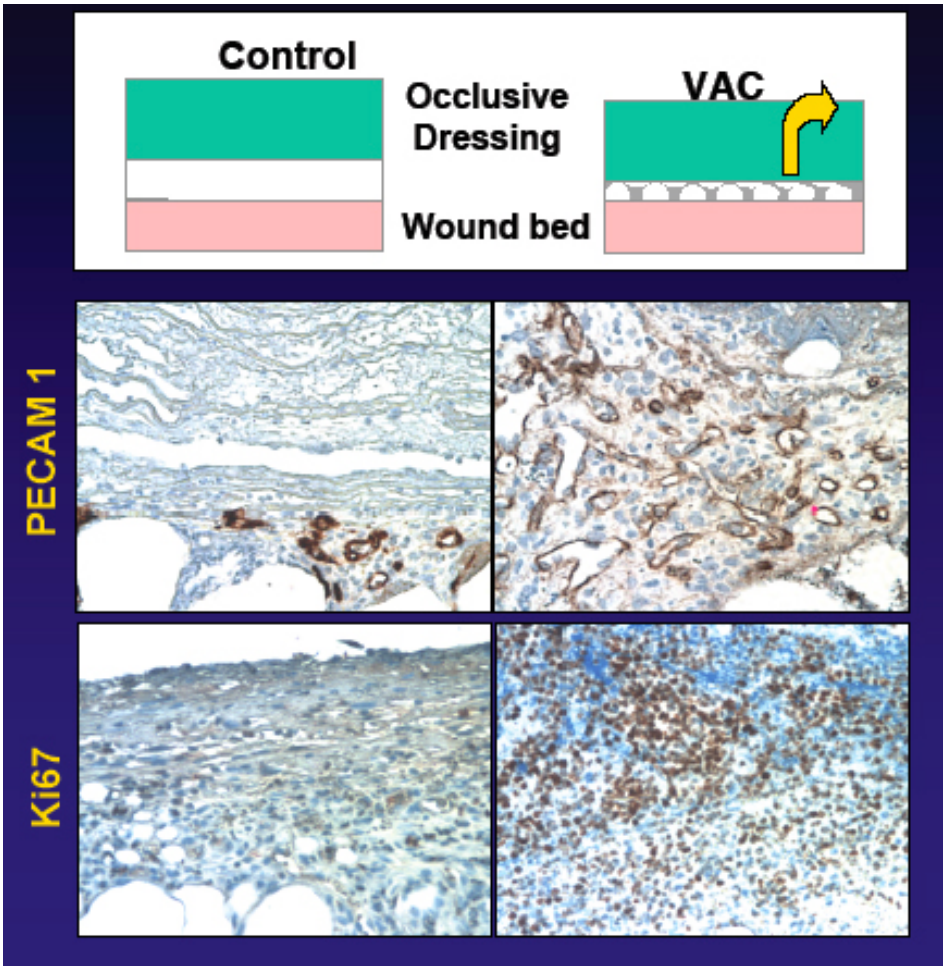

Figure 21. Healing modulation induced by the VAC device.

Combined Approaches.

Improved scaffold design and angiogenetic properties. Scaffolds grafted on full-thickness wounds did not appear to stimulate cell proliferation and tended to slow wound vascularization compared to ungrafted controls (Fig. 15). Since the structure of the scaffolds appear to represent a physical barrier to revascularization, scaffolds were micronized, preserving the regenerative properties (pore size, chemical composition, randomly organized collagen, while allowing for more conformability. Micronized scaffolds, freeze-dried with PRP, stimulated revascularization ($p<0.05$) compared to ungrafted wounds (Fig. 22), noticeably improving the limitation of solid acellular scaffolds.

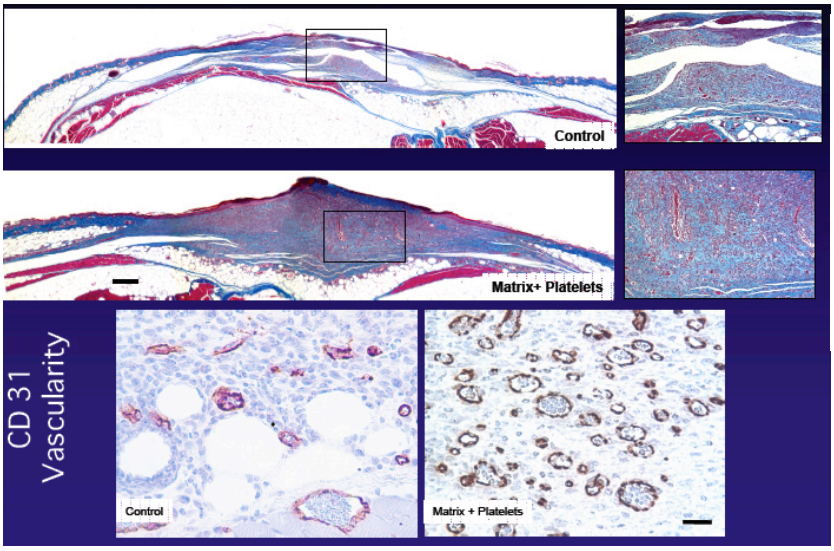

Figure 22. Micronized scaffolds combined with PRP show increased angiogenesis.

Optimization of the application of VAC device. Clinically, the VAC device is applied continuously for periods from days to entire weeks. Since the analysis of the effects of the forces using the rat ear stretch model emphasized that cyclical regimens stimulate cell proliferation more rapidly than continuous, and that the most dramatic increases happen awithin a few hours from the initiation of the stimulation, we customized the application of the VAC. Intriguingly, results show that it was possible to induce comparable increases in cell proliferation to 7days, continuous application of the VAC (168 hours), just with an initial stimulation of 12hours, or when the application was cycled (3 times x 4 hours, Fig. 23). These findings are clinically relevant, as they may shorten the time needed to heal wounds and hospital stay length.

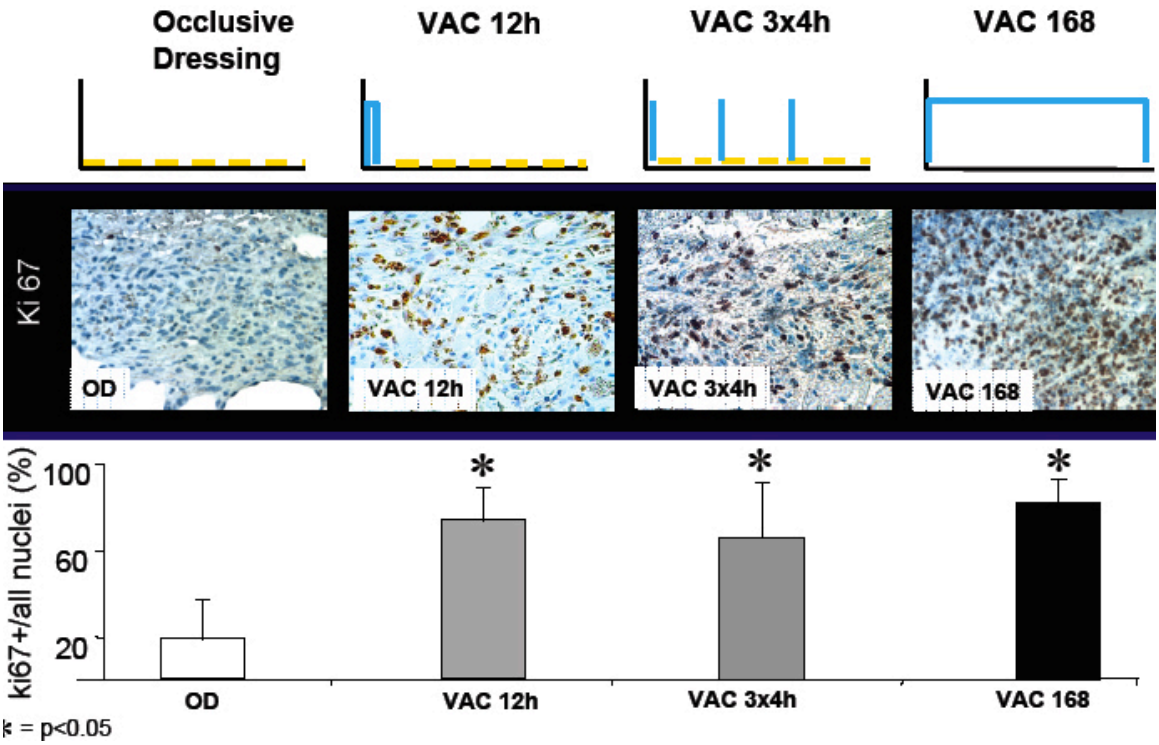

Figure 23. Optimization of the force profile in VAC teraphy. *=p<0.05

NAG scaffold and VAC therapy. Being the NAG a highly angiogenic polymer, its fibers were used to generate a scaffold with regenerative properties (similar to collagen-gag scaffolds) to overcome the typical scaffold limitations. To further stimulate cell proliferation, the VAC therapy was applied as dressing on top of the scaffold with an optimized pattern of application (12 hours). Results show on day 7, highly vascularized and proliferating scaffolds (Fig. 24).

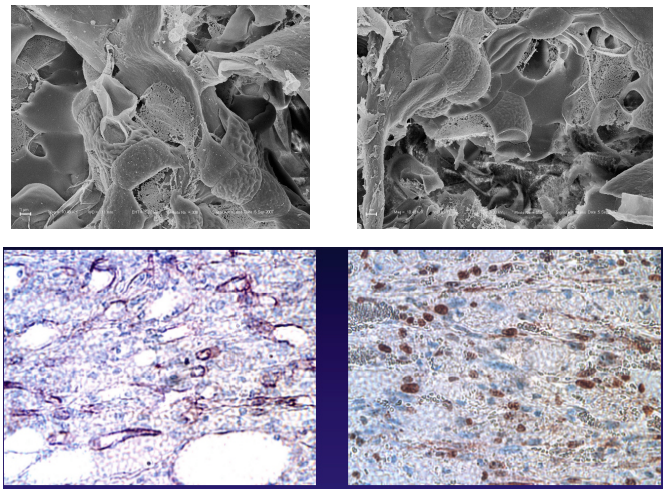

Figure 24. Top: NAG scaffolds in SEM. Randomly oriented fibers and red blood cells can be noted. **Bottom:** the NAG scaffold under VAC therapy stimulated both proliferation and angiogenesis.

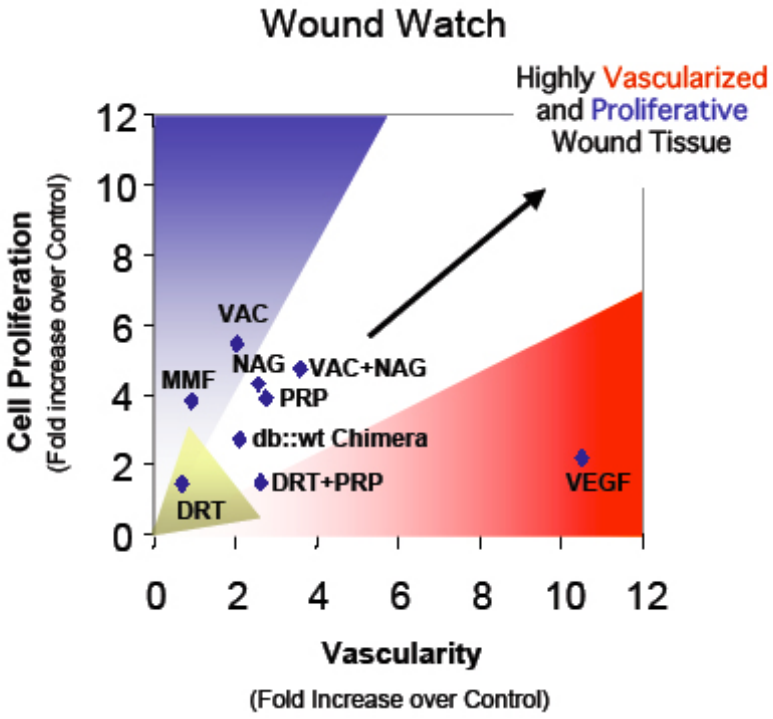

Figure 25. The Wound Watch Staging System: summary of the results of the study. In this study, a novel wound healing staging system was created (wound watch), based on wound vascularity and proliferation. Wounds, in order to heal properly, need a balanced stimulation of both parameters. Stimuli may derive from circulation, as shown in db-chimera wounds, which showed enhanced healing compared to db-controls in the parabiotic model.
Results show that the cardinal elements of the wound healing paradigm induce, alone, an umbalanced stimulation. While VEGF stimulated angiogenesis (red zone), MMFs and VAC triggered mainly cell proliferation (blue zone) and DRTs (needed to guide wound regeneration instead of repair) do not stimulate any of the healing parameters (golden area).
Combinatorial approaches, such as DRTs with improved design and chemical composition and in combination with MMF (DRT+PRP, VAC+NAG), show enhanced healing effects stimulating harmonically both parameters.
Legend: MMF=Micro Mechanical Forces; DRT=Dermal Regeneration Template (collagen-GAG matrix); NAG=Poly-N-AcetylGlucosamine; PRP=Platelet Rich Plasma; VAC= Vacuum Assisted Closure Device.

Figure 26. The new wound healing paradigm was also applied on a patient suffering from purpura fulminans and candidate to lower limb amputation. After aggressive debridement of the lesion, autologous PRP, collagen-GAG matrices and VAC therapy in combination were able to completely rescue the situation, allowing for the salvage of the foot.

5. Discussion

In these studies, we (1) developed novel animal models to study wound healing, including parabiotic and cell stretch models in vivo. (2) Three main approaches were studied: soluble and growth factors, extracellular matrix substitutes and micromechanical forces. For the characterization and comparison of the effects of the healing strategies, we developed (3) a novel wound healing staging system, based on the quantification of cell proliferation and vascularity that we called the *wound watch*. (4) We found that each approach individually induced a characteristic stimulation of healing, but (5) combinatorial approaches reached synergistic effects and represent a novel paradigm in wound healing.

The diabetic mouse served as clinically relevant model of impaired wound healing.[142] The phenotype of this animal resembles diabetes type 2 in humans,[2, 3] in which the stimulation of angiogenesis is crucial for triggering wound repair.[4]

Diabetic cells fail to produce adequate levels of growth factors.[4] Although PDGF, TGF-β, VEGF, EGF, KGF and IGF are crucial in orchestrating wound healing and have been shown to be reduced in diabetic wounds,[5-8] they may not be sufficient to guide repair.

Clinical attempts to treat diabetic patients with lower extremity ulcers by mean of metabolic control or ad hoc replacements of growth factors and cytokines have not met the goal of consistent improvement in wound healing.[4, 9] The success of the parabiotic model for improving diabetic wound healing, in contrast to single-factor interventions,[143] likely reflects the involvement in wound repair of complex cellular interactions and global communication between tissues. Using this model, by exposing diabetic wounds to physiological levels of Wt cells and factors, we identified a key role of modulation of inflammation in improving angiogenesis and ultimately healing. In the wound bed, the engraftment of leukocytes was increased in diabetic chimeras when compared to diabetic controls, and was normalized when compared to wild type animals. However, in diabetic chimeras, wounds showed a direct wild type cell engraftment corresponding to at most 20% of the total cells (not shown). Thus, wild type cells *never* outnumbered diabetic cells in diabetic wounds suggesting a more complex, positive modulatory effect of these wild-type cells on diabetic cells, rather than simply a direct contribution of wild-type cells to wound

healing by replacement of impaired diabetic cells. Our results suggest that the exposure to a wild-type circulation appears to at least partially rescue the function of diabetic inflammatory cells and thereby accelerate the rate of repair, as assessed by multiple morphological and histological parameters. The improved inflammatory response in db animals joined to wt partners may be facilitated by improved angiogenesis at the wound site in these chimeric animals.

In the circulation, diabetic chimeras showed a relative decrease in the levels of mature neutrophils and an increase in circulating B cells, revealing interesting similarities between aging and diabetic individuals. Previous studies have demonstrated an age-dependent deficit in the ability of transplanted hematopoietic stem cells (HSC) from old mice to give rise to peripheral B-lymphocytes, coincident with an increased myelopoietic activity [144]. These findings parallel results from the circulation of diabetic animals in this study, which showed increased representation of neutrophils and decreased representation of B cells. Thus, it is interesting to speculate that alterations in peripheral blood leukocyte subsets in diabetic animals may result from alterations in hematopoietic stem cell function similar to those observed with aging, although additional studies clearly will be required to further understand the importance of these similarities in the two distinct patient populations, both of which are characterized by some degree of healing impairment.[145]

We were surprised to see no changes in glycaemia as a consequence of parabiosis, despite clear evidence of cross-circulation in parabiotic chimeras. Glucose was selected as most relevant metabolic parameter in diabetes. Blood glucose was not altered by parabiotic chimerism, and remained, under any parabiotic condition, high in diabetic animals and within the normal range in wild type animals. These results indicate that the primary mechanism by which parabiotic exposure to circulating factors in a normal mouse reverses impairments in diabetic wound healing is not via normalization of diabetic metabolism. Instead, rescue of diabetic wound healing in the parabiotic model is associated with normalization of circulating leukocyte frequencies and an improved efficiency of inflammatory cell recruitment and angiogenesis in the wound site.

Although growth factors are necessary for wound repair, the addition of recombinant VEGF stimulated only angiogenesis but not cell proliferation, suggesting a non efficient increase in immature blood vessels. It has been shown that platelets and their growth factors stimulate angiogenesis and actively participate in new blood vessel formation.[146] Results from this study suggest that neovascularization and cell proliferation were more harmonically stimulated when wounds were exposed to PRP compared to VEGF. Similar results to the ones achieved with the use of PRP were obtained with the poly-NAG patch, which represents a more promising, device-like approach for treating recalcitrant wounds.

While scaffolds are needed to guide tissue regeneration, they did not appear to stimulate healing, particularly in terms of angiogenesis. Collagen-GAG scaffolds seemed to impair physically the ingrowth of blood vessels from the underside of the matrix and did not recruit circulating endothelial or endothelial progenitor cells. Early vascularization and cellularization are important events after treatment with matrix-based materials or other tissue fillers to reduce bioburden susceptibility since infection is considered a principle problem associated with such avascular materials.[43] When scaffolds were micronized and combined with freeze-dried platelets tended to stimulate revascularization over untreated wounds.

We characterized the response of perfused mammalian ear tissues subjected to different regimens of mechanical forces motivated by the question of how controlled application of tension promotes may be exploited to promote wound healing. We found that tension induced increases in vascular area and epidermal cell proliferation, which are both critical for enhanced repair of tissue defects.

Our experiments show the possibility of predictably harnessing the stimulatory effects of mechanical forces on wound healing *in vivo*, within a few hours or few days from the start of stimulation. Over days, results suggest that increasing force amplitudes – until tissue damage – induced higher stimulation in shorter time. At early times (< 8 hr), the blood vessels of ears subjected to cyclical loads increased in diameter compared to those in sham ears, while continuous tension did not induce significant changes.

Tissues appeared to react more promptly to cyclical force regimens. More studies will be needed to determine the mechano-transduction mechanism in skin but in other tissues such as vasculature, cyclic forces are more effective in influencing genetic expression.[147] Optimization of waveform, may induce quicker and ultimately higher levels of cell proliferation and tissue vascularization when applied to wounds.

Rat ears are complex anatomical structures consisting of epithelium, dermis, fat tissue, muscle and cartilage. These heterogeneous tissue components have different mechanical proprieties, and most likely respond in distinct ways to force application. We were surprised not to be able to measure more of a proliferative response in fibroblasts or endothelial cells. It might be that the extracellular matrix shields these cells somewhat from the mechanical signals perhaps by deformation of the collagen matrix.[141]

A series of *in vitro* work over the past few decades have established the relationship between cell shape distortion and the regulation of its growth and function.[17-19] It is likely that the mechanical forces played an important role in inducing epithelial cell proliferation. Mechanical deformation of the keratinocytes may have stimulated cell growth by altering biochemical signaling responses within the cell, as demonstrated in many studies with cultured cells.[115]

Devices that induce deformations on wound beds, such as microdeformation wound therapy, may directly stimulate dermal cell proliferation[132] promoting granulation tissue formation. New strategies for accelerating wound healing based on the use of mechanical forces, and surgical techniques such as tissue expansion and distraction osteogenesis, would greatly benefit from the optimization of the force characteristics and distributions.

Results showed that the VAC device achieved the highest levels of stimulation of cell proliferation that correlated to the micro-deformation of the wound tissues. The stimulation of angiogenesis induced by the device was, on the other hand, more likely related to an aspecific foreign body reaction due to the polyurethan foam interface.
The strong stimulation induced by the VAC device induced tissue ingrowth into the foam interface. At every dressing change, this newly formed tissue was invariably

removed, causing the loss of vital tissues. This made us develop a biodegradable interface with regenerative properties, based on the NAG polymer. This interface allowed for the transmission of the mechanical forces under the suction force of the VAC system and induction of tissue regeneration due to the architectural and chemical composition. Wounds treated with the modified VAC-NAG combination showed and harmonic stimulation of both vascularity and proliferation, representing the more complete and promising approach for difficult to treat wounds achieved with this study.

The biodegradation rate of this NAG material is undoubtedly affected by the fiber geometry and other factors such as fiber orientation, solubility and cross-linking. Better understanding of how to modulate the foreign body reaction may be useful in designing optimized clinical applications of this material.

6. Conclusions

These results show that a combination of **soluble factors**, **extracellular matrices** and **micro mechanical forces** represents the newest wound healing paradigm. Soluble factors are able to stimulate vascularization, while tension on perfused tissues determines an amplitude and waveform dependent proliferative response. Scaffolds guide wound regeneration rather than repair and can be optimized and variably combined to soluble factos and micro mechanical forces to also trigger a stronger proliferative and vascular response, crucial for improving their clinical performance. We hope that these in vivo results will facilitate the development of novel surgical techniques and devices.

7. Bibliography

1. Yannas IV. *Tissue and Organ Regeneration in Adults*. Springler-Verlag: New York, 2001.
2. Cotran RS, Kumar V, Collins T, Robbins SL. *Robbins pathologic basis of disease* (6th edn). Saunders: Philadelphia, 1999; xv, 1424 p.
3. Singh N, Armstrong DG, Lipsky BA. Preventing foot ulcers in patients with diabetes. *Jama* 2005;**293**(2): 217-228.
4. Campbell LV, Graham AR, Kidd RM, Molloy HF, O'Rourke SR, Colagiuri S. The lower limb in people with diabetes. Position statement of the Australian Diabetes Society. *Med J Aust* 2000;**173**(7): 369-372.
5. Ito M, Liu Y, Yang Z, Nguyen J, Liang F, Morris RJ, Cotsarelis G. Stem cells in the hair follicle bulge contribute to wound repair but not to homeostasis of the epidermis. *Nature medicine* 2005;**11**(12): 1351-1354.
6. Watt FM. Epidermal stem cells: markers, patterning and the control of stem cell fate. *Philosophical transactions of the Royal Society of London* 1998;**353**(1370): 831-837.
7. Levy V, Lindon C, Zheng Y, Harfe BD, Morgan BA. Epidermal stem cells arise from the hair follicle after wounding. *Faseb J* 2007.
8. Tonnesen MG, Feng X, Clark RA. Angiogenesis in wound healing. *The journal of investigative dermatology Symposium proceedings / the Society for Investigative Dermatology, Inc* 2000;**5**(1): 40-46.
9. Lorenz HP, Longaker MT. Wound Healing: repair biology and wound and scar treatment. In: *Plastic Surgery*, Mathes SJ (ed). Saunders Elsevier: Philadelphia, PI, 2006; 209-234.
10. Singer AJ, Clark RA. Cutaneous wound healing. *N Engl J Med* 1999;**341**(10): 738-746.
11. Broughton G, 2nd, Janis JE, Attinger CE. Wound healing: an overview. *Plast Reconstr Surg* 2006;**117**(7 Suppl): 1e-S-32e-S.
12. Broughton G, 2nd, Janis JE, Attinger CE. The basic science of wound healing. *Plast Reconstr Surg* 2006;**117**(7 Suppl): 12S-34S.
13. Peled Z, Galiano RG, Longaker MT. Wound Healing. In: *Handbook of Plastic Surgery*, Greer SE, Benhaim P, Lorenz HP, Chang J, Hedrick MH (eds). Marcel Dekker: New York, NY, 2004.
14. Woolf N. *Anatomia Patologica*. EdiSES: Napoli, 2001.
15. Mustoe TA, O'Shaughnessy K, Kloeters O. Chronic wound pathogenesis and current treatment strategies: a unifying hypothesis. *Plast Reconstr Surg* 2006;**117**(7 Suppl): 35S-41S.
16. Sparkman R. The healing of surgical wounds. In: Sparkman R, editor. Symposia on wound healing; 1985; Pearl River - New York; 1985.
17. Hansen SL, Mathes SJ. Problem wounds and principles of closure. In: *Plastic Surgery*, Mathes SJ (ed). Saunders Elsevier: Philadelphia, PI, 2006; 901-1032.
18. Harding KG, Morris HL, Patel GK. Science, medicine and the future: healing chronic wounds. *BMJ (Clinical research ed* 2002;**324**(7330): 160-163.
19. Natarajan S, Williamson D, Stiltz AJ, Harding K. Advances in wound care and healing technology. *American journal of clinical dermatology* 2000;**1**(5): 269-275.
20. Attinger C, Bulan EJ, Blume PA. Pharmacologic and Mechanical Management of Wounds. In: *Plastic Surgery*, Mathes SJ (ed). Saunders Elsevier: Philadelphia, PI, 2006; 863-900.

21. Martinowitz U, Spotnitz WD. Fibrin tissue adhesives. *Thromb Haemost* 1997;**78**(1): 661-666.
22. Folkman J, Browder T, Palmblad J. Angiogenesis research: guidelines for translation to clinical application. *Thromb Haemost* 2001;**86**(1): 23-33.
23. Galiano RD, Tepper OM, Pelo CR, Bhatt KA, Callaghan M, Bastidas N, Bunting S, Steinmetz HG, Gurtner GC. Topical vascular endothelial growth factor accelerates diabetic wound healing through increased angiogenesis and by mobilizing and recruiting bone marrow-derived cells. *Am J Pathol* 2004;**164**(6): 1935-1947.
24. Kirchner LM, Meerbaum SO, Gruber BS, Knoll AK, Bulgrin J, Taylor RA, Schmidt SP. Effects of vascular endothelial growth factor on wound closure rates in the genetically diabetic mouse model. *Wound Repair Regen* 2003;**11**(2): 127-131.
25. Wieman TJ. Clinical efficacy of becaplermin (rhPDGF-BB) gel. Becaplermin Gel Studies Group. *Am J Surg* 1998;**176**(2A Suppl): 74S-79S.
26. Beer HD, Longaker MT, Werner S. Reduced expression of PDGF and PDGF receptors during impaired wound healing. *J Invest Dermatol* 1997;**109**(2): 132-138.
27. Lauer G, Sollberg S, Cole M, Flamme I, Sturzebecher J, Mann K, Krieg T, Eming SA. Expression and proteolysis of vascular endothelial growth factor is increased in chronic wounds. *J Invest Dermatol* 2000;**115**(1): 12-18.
28. Marikovsky M, Vogt P, Eriksson E, Rubin JS, Taylor WG, Joachim S, Klagsbrun M. Wound fluid-derived heparin-binding EGF-like growth factor (HB-EGF) is synergistic with insulin-like growth factor-I for Balb/MK keratinocyte proliferation. *J Invest Dermatol* 1996;**106**(4): 616-621.
29. Eppley BL, Woodell JE, Higgins J. Platelet quantification and growth factor analysis from platelet-rich plasma: implications for wound healing. *Plast Reconstr Surg* 2004;**114**(6): 1502-1508.
30. Bhanot S, Alex JC. Current applications of platelet gels in facial plastic surgery. *Facial Plast Surg* 2002;**18**(1): 27-33.
31. Knighton DR, Ciresi KF, Fiegel VD, Austin LL, Butler EL. Classification and treatment of chronic nonhealing wounds. Successful treatment with autologous platelet-derived wound healing factors (PDWHF). *Ann Surg* 1986;**204**(3): 322-330.
32. Margolis DJ, Kantor J, Santanna J, Strom BL, Berlin JA. Effectiveness of platelet releasate for the treatment of diabetic neuropathic foot ulcers. *Diabetes Care* 2001;**24**(3): 483-488.
33. Frechette JP, Martineau I, Gagnon G. Platelet-rich plasmas: growth factor content and roles in wound healing. *J Dent Res* 2005;**84**(5): 434-439.
34. Krupski WC, Reilly LM, Perez S, Moss KM, Crombleholme PA, Rapp JH. A prospective randomized trial of autologous platelet-derived wound healing factors for treatment of chronic nonhealing wounds: a preliminary report. *J Vasc Surg* 1991;**14**(4): 526-532; discussion 532-526.
35. Stacey MC, Mata SD, Trengove NJ, Mather CA. Randomised double-blind placebo controlled trial of topical autologous platelet lysate in venous ulcer healing. *Eur J Vasc Endovasc Surg* 2000;**20**(3): 296-301.
36. Steed D, Goslen B, Hambley R, Abell E, Hebda P, Webster M. Clinical trials with purified platelet releasate. *Prog Clin Biol Res* 1991;**365**: 103-113.
37. Steed DL, Goslen JB, Holloway GA, Malone JM, Bunt TJ, Webster MW. Randomized prospective double-blind trial in healing chronic diabetic foot ulcers. CT-102 activated platelet supernatant, topical versus placebo. *Diabetes Care* 1992;**15**(11): 1598-1604.
38. Murphy S. Platelet storage for transfusion. *Semin Hematol* 1985;**22**(3): 165-177.

39. Vournakis JN, Demcheva M, Whitson A, Guirca R, Pariser ER. Isolation, purification, and characterization of poly-N-acetyl glucosamine use as a hemostatic agent. *J Trauma* 2004;**57**(1 Suppl): S2-6.
40. Najjar SF, Healey NA, Healey CM, McGarry T, Khan B, Thatte HS, Khuri SF. Evaluation of poly-N-acetyl glucosamine as a hemostatic agent in patients undergoing cardiac catheterization: a double-blind, randomized study. *J Trauma* 2004;**57**(1 Suppl): S38-41.
41. Fazio VW, Cohen Z, Fleshman JW, van Goor H, Bauer JJ, Wolff BG, Corman M, Beart RW, Jr., Wexner SD, Becker JM, Monson JR, Kaufman HS, Beck DE, Bailey HR, Ludwig KA, Stamos MJ, Darzi A, Bleday R, Dorazio R, Madoff RD, Smith LE, Gearhart S, Lillemoe K, Gohl J. Reduction in adhesive small-bowel obstruction by Seprafilm adhesion barrier after intestinal resection. *Dis Colon Rectum* 2006;**49**(1): 1-11.
42. Pena Ede L, Sala S, Rovira JC, Schmidt RF, Belmonte C. Elastoviscous substances with analgesic effects on joint pain reduce stretch-activated ion channel activity in vitro. *Pain* 2002;**99**(3): 501-508.
43. Orgill DP, Straus FH, 2nd, Lee RC. The use of collagen-GAG membranes in reconstructive surgery. *Ann N Y Acad Sci* 1999;**888**: 233-248.
44. Malette WG, Quigley HJ, Gaines RD, Johnson ND, Rainer WG. Chitosan: a new hemostatic. *Ann Thorac Surg* 1983;**36**(1): 55-58.
45. Fischer TH, Connolly R, Thatte HS, Schwaitzberg SS. Comparison of structural and hemostatic properties of the poly-N-acetyl glucosamine Syvek Patch with products containing chitosan. *Microsc Res Tech* 2004;**63**(3): 168-174.
46. Thatte HS, Zagarins S, Khuri SF, Fischer TH. Mechanisms of poly-N-acetyl glucosamine polymer-mediated hemostasis: platelet interactions. *J Trauma* 2004;**57**(1 Suppl): S13-21.
47. Thatte HS, Zagarins SE, Amiji M, Khuri SF. Poly-N-acetyl glucosamine-mediated red blood cell interactions. *J Trauma* 2004;**57**(1 Suppl): S7-12.
48. Fischer TH, Thatte HS, Nichols TC, Bender-Neal DE, Bellinger AD, Vournakis JN. Synergistic platelet integrin signaling and factor XII activation in poly-N-acetyl glucosamine fiber-mediated hemostasis. *Biomaterials* 2005;**26**(27): 5433-5443.
49. Valeri CR, Srey R, Tilahun D, Ragno G. In vitro effects of poly-N-acetyl glucosamine on the activation of platelets in platelet-rich plasma with and without red blood cells. *J Trauma* 2004;**57**(1 Suppl): S22-25; discussion S25.
50. Browder T, Folkman J, Pirie-Shepherd S. The hemostatic system as a regulator of angiogenesis. *J Biol Chem* 2000;**275**(3): 1521-1524.
51. Kisucka J, Butterfield CE, Duda DG, Eichenberger SC, Saffaripour S, Ware J, Ruggeri ZM, Jain RK, Folkman J, Wagner DD. Platelets and platelet adhesion support angiogenesis while preventing excessive hemorrhage. *Proc Natl Acad Sci U S A* 2006;**103**(4): 855-860.
52. Wright DE, Wagers AJ, Gulati AP, Johnson FL, Weissman IL. Physiological migration of hematopoietic stem and progenitor cells. *Science* 2001;**294**(5548): 1933-1936.
53. Coleman DL, Hummel KP. Effects of parabiosis of normal with genetically diabetic mice. *Am J Physiol* 1969;**217**(5): 1298-1304.
54. Fruhbeck G, Gomez-Ambrosi J. Rationale for the existence of additional adipostatic hormones. *Faseb J* 2001;**15**(11): 1996-2006.
55. Yannas IV. Facts and theories of induced organ regeneration. *Advances in biochemical engineering/biotechnology* 2005;**93**: 1-38.

56. Yannas IV. Similarities and differences between induced organ regeneration in adults and early foetal regeneration. *Journal of the Royal Society, Interface / the Royal Society* 2005;**2**(5): 403-417.
57. Yannas IV, Burke JF, Warpehoski M, Stasikelis P, Skrabut EM, Orgill D, Giard DJ. Prompt, long-term functional replacement of skin. *Transactions - American Society for Artificial Internal Organs* 1981;**27**: 19-23.
58. Yannas IV. *Tissue and Organ Regeneration in Adults* Springer-Verlag New York, Inc.: New York, 2001.
59. Ophof R, Maltha JC, Von den Hoff JW, Kuijpers-Jagtman AM. Histologic evaluation of skin-derived and collagen-based substrates implanted in palatal wounds. *Wound Repair Regen* 2004;**12**(5): 528-538.
60. Levy D, et al. Cymetra: A Treatment Option for Refractory Ulcers. *Wounds* 2004;**16**(12): 359-363.
61. Banta MN, Eaglstein WH, Kirsner RS. Healing of refractory sinus tracts by dermal matrix injection with Cymetra. *Dermatol Surg* 2003;**29**(8): 863-866.
62. Lorber M, Milobsky SA. Stretching of the skin in vivo. A method of influencing cell division and migration in the rat epidermis. *The Journal of investigative dermatology* 1968;**51**(5): 395-402.
63. Mackenzie IC. Does toothbrushing affect gingival keratinization? *Proc R Soc Med* 1972;**65**(12): 1127-1131.
64. Mackenzie IC. The effects of frictional stimulation on mouse ear epidermis. I. Cell proliferation. *The Journal of investigative dermatology* 1974;**62**(2): 80-85.
65. Bullough WS, Laurence EB. The control of epidermal mitotic activity in the mouse. *Proceedings of the Royal Society of London Series B, Containing papers of a Biological character* 1960;**151**: 517-536.
66. Francis AJ, Marks R. Factors responsible for dermally induced epidermal hyperplasia. *Archives for dermatological research* 1977;**258**(3): 275-280.
67. Curtis AS, Seehar GM. The control of cell division by tension or diffusion. *Nature* 1978;**274**(5666): 52-53.
68. Squier CA. The stretching of mouse skin in vivo: effect on epidermal proliferation and thickness. *The Journal of investigative dermatology* 1980;**74**(2): 68-71.
69. Squier CA. The effect of stretching on formation of myofibroblasts in mouse skin. *Cell Tissue Res* 1981;**220**(2): 325-335.
70. Brunette DM. Mechanical stretching increases the number of epithelial cells synthesizing DNA in culture. *J Cell Sci* 1984;**69**: 35-45.
71. Austad ED, Pasyk KA, McClatchey KD, Cherry GW. Histomorphologic evaluation of guinea pig skin and soft tissue after controlled tissue expansion. *Plast Reconstr Surg* 1982;**70**(6): 704-710.
72. Olenius M, Dalsgaard CJ, Wickman M. Mitotic activity in expanded human skin. *Plast Reconstr Surg* 1993;**91**(2): 213-216.
73. Austad ED, Thomas SB, Pasyk K. Tissue expansion: dividend or loan? *Plast Reconstr Surg* 1986;**78**(1): 63-67.
74. Johnson TM, Lowe L, Brown MD, Sullivan MJ, Nelson BR. Histology and physiology of tissue expansion. *The Journal of dermatologic surgery and oncology* 1993;**19**(12): 1074-1078.
75. Argenta LC, Marks M W. Principles of Tissue Expansion. In: *Plastic Surgery*, Mathes SJ (ed), vol 1. Saunders Elsevier: Philadelphia, PA, 2006; 539-568.

76. Ilizarov GA. The tension-stress effect on the genesis and growth of tissues. Part I. The influence of stability of fixation and soft-tissue preservation. *Clinical orthopaedics and related research* 1989(238): 249-281.
77. Gugenheim JJ, Jr. The Ilizarov method. Orthopedic and soft tissue applications. *Clinics in plastic surgery* 1998;**25**(4): 567-578.
78. Lerner A, Ullmann Y, Stein H, Peled IJ. Using the Ilizarov external fixation device for skin expansion. *Annals of plastic surgery* 2000;**45**(5): 535-537.
79. Cherry GW, Austad E, Pasyk K, McClatchey K, Rohrich RJ. Increased survival and vascularity of random-pattern skin flaps elevated in controlled, expanded skin. *Plast Reconstr Surg* 1983;**72**(5): 680-687.
80. Malata CM, Williams NW, Sharpe DT. Tissue expansion: an overview. *Journal of wound care* 1995;**4**(1): 37-44.
81. Marks MW, Argenta LC, Thornton JW. Rapid expansion: experimental and clinical experience. *Clinics in plastic surgery* 1987;**14**(3): 455-463.
82. De Filippo RE, Atala A. Stretch and growth: the molecular and physiologic influences of tissue expansion. *Plast Reconstr Surg* 2002;**109**(7): 2450-2462.
83. Watt FM. Role of integrins in regulating epidermal adhesion, growth and differentiation. *The EMBO journal* 2002;**21**(15): 3919-3926.
84. Torsoni AS, Constancio SS, Nadruz W, Jr., Hanks SK, Franchini KG. Focal adhesion kinase is activated and mediates the early hypertrophic response to stretch in cardiac myocytes. *Circulation research* 2003;**93**(2): 140-147.
85. Duncan RL, Turner CH. Mechanotransduction and the functional response of bone to mechanical strain. *Calcified tissue international* 1995;**57**(5): 344-358.
86. Hamill OP, McBride DW, Jr. The pharmacology of mechanogated membrane ion channels. *Pharmacological reviews* 1996;**48**(2): 231-252.
87. Vandenburgh HH. Mechanical forces and their second messengers in stimulating cell growth in vitro. *The American journal of physiology* 1992;**262**(3 Pt 2): R350-355.
88. Yano S, Komine M, Fujimoto M, Okochi H, Tamaki K. Mechanical stretching in vitro regulates signal transduction pathways and cellular proliferation in human epidermal keratinocytes. *The Journal of investigative dermatology* 2004;**122**(3): 783-790.
89. Takei T, Mills I, Arai K, Sumpio BE. Molecular basis for tissue expansion: clinical implications for the surgeon. *Plast Reconstr Surg* 1998;**102**(1): 247-258.
90. Silver FH, Siperko LM, Seehra GP. Mechanobiology of force transduction in dermal tissue. *Skin Res Technol* 2003;**9**(1): 3-23.
91. Folkman J, Greenspan HP. Influence of geometry on control of cell growth. *Biochimica et biophysica acta* 1975;**417**(3-4): 211-236.
92. Folkman J, Moscona A. Role of cell shape in growth control. *Nature* 1978;**273**(5661): 345-349.
93. Structure and tensegrity. www.kennethsnelson.net.
94. Ingber DE. Tensegrity I. Cell structure and hierarchical systems biology. *J Cell Sci* 2003;**116**(Pt 7): 1157-1173.
95. Ingber D. How cells (might) sense microgravity. *Faseb J* 1999;**13 Suppl**: S3-15.
96. Wang N, Butler JP, Ingber DE. Mechanotransduction across the cell surface and through the cytoskeleton. *Science (New York, NY* 1993;**260**(5111): 1124-1127.
97. Wang N, Ingber DE. Control of cytoskeletal mechanics by extracellular matrix, cell shape, and mechanical tension. *Biophysical journal* 1994;**66**(6): 2181-2189.

98. Wang N, Ingber DE. Probing transmembrane mechanical coupling and cytomechanics using magnetic twisting cytometry. *Biochemistry and cell biology = Biochimie et biologie cellulaire* 1995;**73**(7-8): 327-335.
99. Maniotis AJ, Chen CS, Ingber DE. Demonstration of mechanical connections between integrins, cytoskeletal filaments, and nucleoplasm that stabilize nuclear structure. *Proceedings of the National Academy of Sciences of the United States of America* 1997;**94**(3): 849-854.
100. Wang N, Naruse K, Stamenovic D, Fredberg JJ, Mijailovich SM, Tolic-Norrelykke IM, Polte T, Mannix R, Ingber DE. Mechanical behavior in living cells consistent with the tensegrity model. *Proceedings of the National Academy of Sciences of the United States of America* 2001;**98**(14): 7765-7770.
101. Ingber DE. Cellular tensegrity: defining new rules of biological design that govern the cytoskeleton. *J Cell Sci* 1993;**104 (Pt 3)**: 613-627.
102. Hubmayr RD, Shore SA, Fredberg JJ, Planus E, Panettieri RA, Jr., Moller W, Heyder J, Wang N. Pharmacological activation changes stiffness of cultured human airway smooth muscle cells. *The American journal of physiology* 1996;**271**(5 Pt 1): C1660-1668.
103. Stamenovic D, Mijailovich SM, Tolic-Norrelykke IM, Chen J, Wang N. Cell prestress. II. Contribution of microtubules. *American journal of physiology* 2002;**282**(3): C617-624.
104. Wang N, Tolic-Norrelykke IM, Chen J, Mijailovich SM, Butler JP, Fredberg JJ, Stamenovic D. Cell prestress. I. Stiffness and prestress are closely associated in adherent contractile cells. *American journal of physiology* 2002;**282**(3): C606-616.
105. Kolodney MS, Wysolmerski RB. Isometric contraction by fibroblasts and endothelial cells in tissue culture: a quantitative study. *The Journal of cell biology* 1992;**117**(1): 73-82.
106. Kolodney MS, Elson EL. Contraction due to microtubule disruption is associated with increased phosphorylation of myosin regulatory light chain. *Proceedings of the National Academy of Sciences of the United States of America* 1995;**92**(22): 10252-10256.
107. Mizushima-Sugano J, Maeda T, Miki-Noumura T. Flexural rigidity of singlet microtubules estimated from statistical analysis of their contour lengths and end-to-end distances. *Biochimica et biophysica acta* 1983;**755**(2): 257-262.
108. Ruoslahti E. Stretching is good for a cell. *Science (New York, NY* 1997;**276**(5317): 1345-1346.
109. Miyamoto S, Akiyama SK, Yamada KM. Synergistic roles for receptor occupancy and aggregation in integrin transmembrane function. *Science (New York, NY* 1995;**267**(5199): 883-885.
110. McNamee HP, Liley HG, Ingber DE. Integrin-dependent control of inositol lipid synthesis in vascular endothelial cells and smooth muscle cells. *Experimental cell research* 1996;**224**(1): 116-122.
111. Ingber DE. Tensegrity: the architectural basis of cellular mechanotransduction. *Annual review of physiology* 1997;**59**: 575-599.
112. Ingber DE. Tensegrity II. How structural networks influence cellular information processing networks. *J Cell Sci* 2003;**116**(Pt 8): 1397-1408.
113. Chen CS, Mrksich M, Huang S, Whitesides GM, Ingber DE. Geometric control of cell life and death. *Science (New York, NY* 1997;**276**(5317): 1425-1428.
114. Huang S, Chen CS, Ingber DE. Control of cyclin D1, p27(Kip1), and cell cycle progression in human capillary endothelial cells by cell shape and cytoskeletal tension. *Mol Biol Cell* 1998;**9**(11): 3179-3193.

115. Huang S, Ingber DE. The structural and mechanical complexity of cell-growth control. *Nat Cell Biol* 1999;**1**(5): E131-138.
116. Dike LE, Ingber DE. Integrin-dependent induction of early growth response genes in capillary endothelial cells. *J Cell Sci* 1996;**109 (Pt 12)**: 2855-2863.
117. www.idf.org/home/index.cfm.
118. Parker KK, Brock AL, Brangwynne C, Mannix RJ, Wang N, Ostuni E, Geisse NA, Adams JC, Whitesides GM, Ingber DE. Directional control of lamellipodia extension by constraining cell shape and orienting cell tractional forces. *Faseb J* 2002;**16**(10): 1195-1204.
119. Argenta LC, Morykwas MJ, Marks MW, DeFranzo AJ, Molnar JA, David LR. Vacuum-assisted closure: state of clinic art. *Plast Reconstr Surg* 2006;**117**(7 Suppl): 127S-142S.
120. Greene AK, Puder M, Roy R, Arsenault D, Kwei S, Moses MA, Orgill DP. Microdeformational wound therapy: effects on angiogenesis and matrix metalloproteinases in chronic wounds of 3 debilitated patients. *Ann Plast Surg* 2006;**56**(4): 418-422.
121. Smith A (ed). *V.A.C. Therapy clinical guidelines*. KCI Lincensing Inc.: San Antonio, Texas, 2006.
122. Argenta LC, Morykwas MJ. Vacuum-assisted closure: a new method for wound control and treatment: clinical experience. *Annals of plastic surgery* 1997;**38**(6): 563-576; discussion 577.
123. Philbeck TE, Jr., Whittington KT, Millsap MH, Briones RB, Wight DG, Schroeder WJ. The clinical and cost effectiveness of externally applied negative pressure wound therapy in the treatment of wounds in home healthcare Medicare patients. *Ostomy/wound management* 1999;**45**(11): 41-50.
124. Evans D, Land L. Topical negative pressure for treating chronic wounds: a systematic review. *British journal of plastic surgery* 2001;**54**(3): 238-242.
125. Braakenburg A, Obdeijn MC, Feitz R, van Rooij IA, van Griethuysen AJ, Klinkenbijl JH. The clinical efficacy and cost effectiveness of the vacuum-assisted closure technique in the management of acute and chronic wounds: a randomized controlled trial. *Plast Reconstr Surg* 2006;**118**(2): 390-397; discussion 398-400.
126. Moues CM, Vos MC, van den Bemd GJ, Stijnen T, Hovius SE. Bacterial load in relation to vacuum-assisted closure wound therapy: a prospective randomized trial. *Wound Repair Regen* 2004;**12**(1): 11-17.
127. Venturi ML, Attinger CE, Mesbahi AN, Hess CL, Graw KS. Mechanisms and clinical applications of the vacuum-assisted closure (VAC) Device: a review. *American journal of clinical dermatology* 2005;**6**(3): 185-194.
128. Genecov DG, Schneider AM, Morykwas MJ, Parker D, White WL, Argenta LC. A controlled subatmospheric pressure dressing increases the rate of skin graft donor site reepithelialization. *Annals of plastic surgery* 1998;**40**(3): 219-225.
129. Miller Q, Bird E, Bird K, Meschter C, Moulton MJ. Effect of subatmospheric pressure on the acute healing wound. *Current Surgery* 2004;**61**(2): 205-208.
130. Morykwas MJ, Simpson J, Punger K, Argenta A, Kremers L, Argenta J. Vacuum-assisted closure: state of basic research and physiologic foundation. *Plast Reconstr Surg* 2006;**117**(7 Suppl): 121S-126S.
131. Mendonca DA, Papini R, Price PE. Negative-pressure wound therapy: a snapshot of the evidence. In; 2006. p. 261-271.
132. Saxena V, Hwang CW, Huang S, Eichbaum Q, Ingber D, Orgill DP. Vacuum-assisted closure: microdeformations of wounds and cell proliferation. *Plast Reconstr Surg* 2004;**114**(5): 1086-1096; discussion 1097-1088.

133. Jacobi J, Jang JJ, Sundram U, Dayoub H, Fajardo LF, Cooke JP. Nicotine accelerates angiogenesis and wound healing in genetically diabetic mice. *The American journal of pathology* 2002;**161**(1): 97-104.
134. Michaels Jt, Dobryansky M, Galiano RD, Bhatt KA, Ashinoff R, Ceradini DJ, Gurtner GC. Topical vascular endothelial growth factor reverses delayed wound healing secondary to angiogenesis inhibitor administration. *Wound Repair Regen* 2005;**13**(5): 506-512.
135. Maloney BP, Murphy BA, Cole HP, 3rd. Cymetra. *Facial Plast Surg* 2004;**20**(2): 129-134.
136. ME B. Technical Manual. 14 ed. Bethesda, MD: American Association of Blood Banks
2002.
137. Pietramaggiori G, Kaipainen A, Czeczuga JM, Wagner CT, Orgill DP. Freeze-dried platelet-rich plasma shows beneficial healing properties in chronic wounds. *Wound Repair Regen* 2006;**14**(5): 573-580.
138. Saldalamacchia G, Lapice E, Cuomo V, De Feo E, D'Agostino E, Rivellese AA, Vaccaro O. A controlled study of the use of autologous platelet gel for the treatment of diabetic foot ulcers. *Nutr Metab Cardiovasc Dis* 2004;**14**(6): 395-396.
139. Sanders R. Torsional elasticity of human skin in vivo. *Pflugers Arch* 1973;**342**(3): 255-260.
140. Pietramaggiori A, Kaipainen A, Ho D, Orser C, Pebley W, Rudolph A, DP. O. Trehalose lyophilized platelets for wound healing. *Wound Repair Regen* 2006(in press).
141. Wilhelmi BJ, Blackwell SJ, Mancoll JS, Phillips LG. Creep vs. stretch: a review of the viscoelastic properties of skin. *Ann Plast Surg* 1998;**41**(2): 215-219.
142. Greenhalgh DG. Models of wound healing. *J Burn Care Rehabil* 2005;**26**(4): 293-305.
143. Steed DL. Clinical evaluation of recombinant human platelet-derived growth factor for the treatment of lower extremity ulcers. *Plast Reconstr Surg* 2006;**117**(7 Suppl): 143S-149S; discussion 150S-151S.
144. Rossi DJ, Bryder D, Zahn JM, Ahlenius H, Sonu R, Wagers AJ, Weissman IL. Cell intrinsic alterations underlie hematopoietic stem cell aging. *Proc Natl Acad Sci U S A* 2005;**102**(26): 9194-9199.
145. Ashcroft GS, Horan MA, Ferguson MW. The effects of ageing on cutaneous wound healing in mammals. *J Anat* 1995;**187 (Pt 1)**: 1-26.
146. Kisucka J, Butterfield CE, Duda DG, Eichenberger SC, Saffaripour S, Ware J, Ruggeri ZM, Jain RK, Folkman J, Wagner DD. Platelets and platelet adhesion support angiogenesis while preventing excessive hemorrhage. *Proc Natl Acad Sci U S A* 2006.
147. Blackman BR, Garcia-Cardena G, Gimbrone MA, Jr. A new in vitro model to evaluate differential responses of endothelial cells to simulated arterial shear stress waveforms. *J Biomech Eng* 2002;**124**(4): 397-407.